Development of Multi-Task Catalysts for Removal of NO_x and Toxic Organic Compounds during Coal Combustion

Final Report

Reporting Period Start Date: September 30, 1997
Reporting Period End Date: September 29, 2001

by

Panagiotis G. Smirniotis and Robert G. Jenkins

Date report was issued: February 4, 2002
DoE Award Number: DE-FG26-97FT97274

Chemical Engineering Department
601 ERC
University of Cincinnati
Cincinnati, OH 45221-0171

DISCLAIMER

No patentable subject matter is disclosed in this report.

TABLE OF CONTENTS

FIGURES AND TABLES

Table 1. Supports used in this study

Table 2. BET areas of the supports used in the present study

Table 3. NO conversion and N_2 selectivity over P25 and WO_3/TiO_2 (W/Ti=5/30) at 400 ^oC loaded with vanadia with and without aging of the vanadium precursor. The catalysts were activated at 400 ^oC for 1.5 hours in oxygen (GHSV=30,000 h^{-1}, NO=2000 ppm, NH_3=2000 ppm, O_2=2000 ppm, time on stream = 2 hours).

Table 4. Ratios of the areas of Brønsted to Lewis peaks (B/L) for the catalysts involved in the present study after they were treated with ammonia (the ratios were formed from the bands at 1427 and 1604 cm^{-1}, respectively). The wafers were heated at 150 ^oC.

Table 5. Physical characteristics of the different supports

Table 6. Composition, metal dispersion, and percentage of mass loss upon calcination for catalysts used in this study for different levels of monolayer coverage and vanadium valence state.

Table 7. XPS surface concentrations for monolayer coverage of V_2O_5 on P25 TiO_2

Table 8. Physical properties of catalysts used in this study

Figure 1. XRD patterns of several TiO_2-based supports. The atomic ratios of the metals are Ti/W=30/5, Ti/Zr=30/5, Ti/Cr=30/5, and Ti/Si/Al=30/2/1.

Figure 2. NO conversion, NH_3 conversion and N_2 selectivity of selected catalysts at 300 ^oC (GHSV=30,000 h^{-1}, NO=2000 ppm, NH_3=2000 ppm, O_2=2000 ppm, time on stream 2 hours). All supports were calcined at 500 ^oC and oxidized for 1.5 hours at 450 ^oC. The aged vanadium oxalate solution was used for all catalysts with the exception of Ti/Si/Al+V(5+)(5w%).

Figure 3. NO conversion versus the reaction temperature over WO_3/TiO_2 (W/Ti=5/30) loaded with different amounts of V_2O_5 (GHSV=30,000 h^{-1}, NO=2000 ppm, NH_3=2000 ppm, O_2=2000 ppm, time on stream 2 hours).

Figure 4. N_2 selectivity versus the reaction temperature over WO_3/TiO_2 (W/Ti=5/30) loaded with different amounts of V_2O_5 (GHSV=30,000 h^{-1}, NO=2000 ppm, NH_3=2000 ppm, O_2=2000 ppm, time on stream=2 hours).

Figure 5. NO conversion versus the reaction temperature over P25 loaded with different amounts of V_2O_5 (GHSV=30,000 h^{-1}, NO=2000 ppm, NH_3=2000 ppm, O_2=2000 ppm, time on stream=2 hours).

Figure 6. N_2 selectivity versus the reaction temperature over P25 loaded with different amounts of V_2O_5 (GHSV=30,000 hr^1, NO=2000 ppm, NH_3=2000 ppm, O_2=2000 ppm, time on stream=2 hours).
Figure 7. Sequenced synthesis of V_2O_5/TiO_2 catalysts

Figure 8. Ti $2p_{3/2}$ and Ti $2p_{1/2}$ peaks for monolayer coverage of different vanadium loading sequences on P25 TiO_2.

Figure 9. V $2p_{3/2}$ peaks for monolayer coverage of different vanadium loading sequences on P25 TiO_2.

Figure 10. Capillary electrophoresis spectrum for aqueous ammonium metavanadate

Figure 11. Spectrum obtained from capillary electrophoresis measurements of the aged vanadium oxalate solution

Figure 12. Catalytic performance of monolayer V_2O_5/TiO_2 catalysts supported on different types of TiO_2 supports at 300°C and 50,000 h^{-1}

Figure 13. Catalytic performance of monolayer coverage of V_2O_5 on Hombikat and Ishihara TiO_2 supports

Figure 14. FT-IR spectra of uncalcined 22.4 wt.% V_2O_5/ Hombikat TiO_2 synthesized by a) V^{+5} or b) V^{+4} recorded at room temperature in helium.

Figure 15. FT-IR spectra of 22.4 wt% V_2O_5/Hombikat TiO_2 synthesized from V^{+4}. a) 150°C, b) 250°C, c) 300°C, d) 350°C (Calcined at 500°C for 2 hours, pretreated for 2 hours at 400°C in helium, all samples cooled to 150°C for data collection)

Figure 16. FT-IR spectra of 22.4 wt% V_2O_5/Hombikat TiO_2 synthesized from V^{+5}. a) 150°C, b) 250°C, c) 300°C (Calcined at 500°C for 2 hours, pretreated for 2 hours at 400°C in helium, all samples cooled to 150°C for data collection)

Figure 17. FT-IR spectra of 7.25 wt% V_2O_5/P25 TiO_2. Initial layer V^{+4}. Final layer V^{+5}. a) 150°C, b) 250°C, c) 300°C (Calcined at 500°C for 2 hours, pretreated for 2 hours at 400°C in helium, all samples cooled to 150°C for data collection)

Figure 18. FT-IR spectra of 7.25 wt% V_2O_5/P25 TiO_2. Initial layer V^{+5}. Final layer V^{+4}. a) 150°C, b) 250°C, c) 300°C, d) 350°C (Calcined at 500°C for 2 hours, pretreated for 2 hours at 400°C in helium, all samples cooled to 150°C for data collection)

Figure 19. FT-IR spectra of 7.25 wt% V_2O_5/P25 TiO_2. Initial layer V^{+4}. Final layer V^{+4}. a) 150°C, b) 250°C, c) 300°C, d) 350°C (Calcined at 500°C for 2 hours, pretreated for 2 hours at 400°C in helium, all samples cooled to 150°C for data collection)

Figure 20. Hydrogen temperature programmed reduction of 22.4 wt% V_2O_5/Hombikat TiO_2 synthesized from V^{+4} and V^{+5}. (50-800°C at 5°C/min, dwell at 800°C for 1 hour)

Figure 21. XRD spectra of single and double monolayer V_2O_5 catalysts.

Figure 22. Raman spectra collected under ambient conditions for (a) 22.4 wt% V_2O_5/Homibat TiO_2 synthesized with V^{+4} and (b) 22.4 wt% V_2O_5/Homibat TiO_2 synthesized with V^{+5}.

Figure 23. Raman spectra collected under ambient conditions of 7 wt% V_2O_5/P25 TiO_2: (a) V^{+5} initial layer, V^{+5} completion of monolayer, (b) V^{+4} initial layer, V^{+5} completion of monolayer, (c) V^{+4} initial layer, V^{+4} completion of monolayer, and (d) V^{+5} initial layer, V^{+4} completion of monolayer.

Figure 24. Distribution of V^{+4} and V^{+5} ions in the aged vanadium oxalate solution over time.

EXECUTIVE SUMMARY

The work performed during this project focused on the identification of materials capable of providing high activity and selectivity for the selective catalytic reduction of nitric oxide with ammonia. The material surface characteristics were correlated with the catalytic behavior of our catalysts to increase our understanding and to help improve the $DeNO_x$ efficiency. The catalysts employed in this study include mixed oxide composite powders (TiO_2-Cr_2O_3, TiO_2-ZrO_2, TiO_2-WO_3, TiO_2-SiO_2, and TiO_2-Al_2O_3) loaded with varying amounts of V_2O_5, along with 5 different commercial sources of TiO_2. V_2O_5 was added to the commercial sources of TiO_2 to achieve monolayer coverage. Since the valence state of vanadium in the precursor solution during the impregnation step significantly impacted catalytic performance, catalysts were synthesized from both V^{+4} and V^{+5} solutions explain this phenomenon.

Specifically, the synthesis of catalysts from V^{5+} precursor solutions yields lower-performance catalysts compared to the case of V^{4+} under identical conditions. Aging the vanadium precursor solution, which is associated with the reduction of V^{5+} to V^{4+} ($VO_2^+ \rightarrow VO^{2+}$), prior to impregnation results in catalysts with excellent catalytic behavior under identical activation and operating conditions. This work also added vanadia to TiO_2-based supports with low crystallinity. These supports, which have traditionally performed poorly, are now able to function as effective SCR catalysts. Increasing the acidity of the support by incorporating oxides such as WO_3 and Al_2O_3 significantly improves the SCR activity and nitrogen selectivity. It was also found that the supports should be synthesized with the simultaneous precipitation of the corresponding precursors. The mixed oxide catalysts possess Brønsted and Lewis acid sites of comparable strength over a wide range of temperatures. Catalysts prepared from aged vanadium precursor solutions also demonstrated a wider temperature window for optimum operation.

A number of V_2O_5/TiO_2 catalysts have been tested to study the effect of vanadium's valence state during synthesis on catalytic performance. Monolayer catalysts were synthesized from five different kinds of TiO_2 supports with varying surface areas and crystalline phase compositions. Catalysts prepared from an aged V^{+4} solution consistently performed better than those prepared from fresh V^{+5} solutions. Both NO conversion and N_2 selectivity were improved through the use of V^{+4}. A number of surface characterization techniques were used to search for differences in the properties of catalysts prepared from the two different methods. Surprisingly, X-ray photoelectron spectroscopy results for uncalcined catalysts actually revealed that the surface vanadium species for catalysts synthesized from the V^{+4} solution behave more like V^{+5} than those species deposited

from the V^{+5} solution. Oxygen chemisorption experiments did not reveal any significant differences in the vanadium valence state used during synthesis and metal dispersion. UV-VIS spectroscopy, capillary electrophoresis, and capillary electrophoresis combined with inductively coupled plasma mass spectroscopy were used in an attempt to quantitatively determine the distribution of vanadium valence states in the aged vanadium oxalate solution. The complexity of the vanadium oxalate solution only allowed qualitative observations to be made. FT-IR showed that catalysts prepared from V^{+4} possessed both Lewis and Brønsted acid sites before the catalyst was exposed to ammonia. In contrast, V^{+5} possessed only Lewis acid sites before exposure to ammonia. Catalysts synthesized from V^{+4} also showed the presence of stronger acid sites compared to V^{+5}. Those catalysts synthesized from V^{+4} still possessed acidity at temperatures above 300°C. H_2 TPR experiments indicated that the reduction of vanadium species deposited as V^{+4} occurs at a lower temperature than vanadium deposited as V^{+5}, suggesting that the increased reducibility of vanadium plays an advantageous role during the redox cycle occurring during this reaction mechanism. Similar to all of the other surface characterization results, Raman spectroscopy revealed no significant differences in the nature of vanadium species present on the surface of the catalysts as a function of the vanadium valence state present during synthesis. Both the stronger acidity and increased reducibility of catalysts synthesized from aged vanadium oxalate solutions (V^{+4}) are believed to contribute higher catalytic activity in the selective catalytic reduction of nitric oxide with ammonia. The potentiometric titration method developed to measure the relative quantities of V^{+3}, V^{+4}, and V^{+5} in the vanadium oxalate solution was ultimately successful at distinguishing between the V^{+4} and V^{+5} species present in the aged vanadium oxalate solution and showed that the aged solutions are stable over time; little change was seen in the concentration of different vanadium species up to approximately 3 years of storage time.

I. THE EFFECT OF VANADIUM VALENCE STATE ON MIXED OXIDE COMPOSITES

ABSTRACT

The work performed during this phase of the project focuses on the screening for effectiveness of the synthesized catalysts. The correlation of the surface properties with the catalytic behavior of our catalysts will increase our understanding and will help us to improve the $DeNO_x$ efficiency. The catalysts employed in this study include mixed oxide composite powders (combinations of TiO_2 (primary oxide), Cr_2O_3, ZrO_2, WO_3, SiO_2, and Al_2O_3) loaded with varying amounts of V_2O_5.

It is remarkable to note that the valence state of vanadium in the precursor solution during the impregnation step is crucial for the synthesis of efficient $DeNO_x$ catalysts. More specifically, V^{5+} in the precursor solution yields lower-performance catalysts compared to the case of V^{4+} under identical conditions. Aging the vanadium precursor solution, which is associated with the reduction of V^{5+} to V^{4+} ($VO_2^+ \rightarrow VO^{2+}$), prior to impregnation results in catalysts with excellent catalytic behavior under identical activation and operating conditions. The present variation of loading vanadia is used for TiO_2-based supports with low crystallinity. These supports, which have traditionally performed poorly, are now able to function as effective SCR catalysts. Increasing the acidity of the support by incorporating oxides such as WO_3 and Al_2O_3 significantly improves the SCR activity and nitrogen selectivity. The concentration of tungsten used in these catalysts was higher than that typically used in industry. It was also found that the supports should be synthesized with the simultaneous precipitation of the corresponding precursors. From our work we found that the mixed oxide catalysts possess Brønsted and Lewis acid sites of comparable strength over a wide range of temperatures. Catalysts prepared from aged vanadium precursor solutions demonstrated a wider temperature window for optimum operation.

1.1 INTRODUCTION

The work discussed in this section focuses on the area of plain NO_x reduction. The work primarily aims at developing, characterizing, and catalytically evaluating novel catalysts for transforming NO_x to molecular nitrogen. The new catalysts are based on a modified vanadia loading procedure developed in our Laboratories for the synthesis of TiO_2-based catalysts. The characterization of the surface properties of the catalysts and the development of correlations between catalytic performance and surface characteristics was performed during the first year of the award. Screening for effectiveness tests were performed during the second year of the award.

This section presents the catalytic performance of several TiO_2-based catalysts doped with one or more metal oxides for the SCR of NO. It was found that the valence of vanadium during the impregnation step significantly impacts catalytic performance. Specifically, aging the precursor solution results in the transformation of $V^{5+} \rightarrow V^{4+}$. This transformation leads to $DeNO_x$ catalysts with superior performance. It is worth noting that catalysts synthesized from supports with a low degree of titania crystallinity using the newly adapted impregnation method, such as $Al_2O_3/SiO_2/TiO_2$ polyoxides, had very good performance.

1.2 EXPERIMENTAL WORK

1.2.1 Catalyst Preparation

Binary oxide supports were prepared by a sol-gel co-precipitation method [Gordon et al., 1959; Vogt et al., 1988; Economidis, et al., 1998] using TiO_2 as the primary oxide and Cr_2O_3, ZrO_2, or WO_3 as the secondary oxide. Ternary $TiO_2/SiO_2/Al_2O_3$ supports were synthesized as well by incorporating aluminum and silicon precursors. The supports were synthesized from the following inorganic precursors: titanium tetrachloride (Aldrich 99%), chromium chloride hexahydrate (Aldrich), zirconium chloride (Aldrich 99.5+ %), ammonium metatungstate hydrate (Aldrich, +80 mesh), aluminum chloride (Alfa reagent grade), and silicon tetrachloride (Aldrich 99%). The procedure first involved the dissolution of the appropriate amount of $TiCl_4$ into a hydrochloric acid solution containing 10 % vol. concentrated HCl. The appropriate amount of precursor for the other metal oxides was dissolved into distilled water and incorporated dropwise into the $TiCl_4$ solution. The atomic ratio of the oxides was Ti:Me=30:5 (where Me stands for Cr, Zr, or W) and Ti:Si:Al=30:2:1 for the case of the ternary oxide, unless specified otherwise. The resulting solution was heated to 65 °C and kept at this temperature for 16 hours under vigorous stirring. After that period the solution was reacted with NH_4OH (typically around 50 ml) to induce precipitation. After precipitation the solution was aged for another 24 hours at room temperature, filtered, and then washed thoroughly with distilled water. The paste was dried overnight at 125 °C. The resulting powder was ground, sieved through an 80-mesh screen, and calcined at the desired temperature. For the catalytic experiments that will be presented in this paper, the supports were calcined in air at 500 °C for 3 hours (Table 1). P25 was provided by Degussa Corporation (T_iO CAS No. 13463-67-7).

Table 1: *Supports used in this study*

Support	Composition (atomic ratio)	Calcination Temperature(°C)	Time(h)
WO_3/TiO_2	W/Ti = 5:30	500	3
P25(Degussa)	Ti = 1	500	3
ZrO_2/TiO_2	Zr/Ti = 5:30	500	3
Cr_2O_3/TiO_2	Cr/Ti = 5:30	500	3
$Al_2O_3/SiO_2/TiO_2$	Al/Si/Ti = 1:2:30	500	3
WO_3/TiO_2	W/Ti = 5:30	500	3

Wet impregnation was used for catalyst synthesis. Catalysts prepared without aging included the support in the preparation (first step) of the vanadium oxalate solution. Aged catalysts were created from vanadium oxalate solutions that were mixed for at least 16 hours before addition (second step) to the support. It should be mentioned that the mass ratio of support to oxalic acid was kept equal to 6 for both methods. In the first step, 100 ml of a 0.0315M solution of ammonium metavanadate (Aldrich 99+ %) and 100 ml of a 0.063M solution of oxalic acid hydrate (Fischer A.C.S. reagent) were vigorously stirred until complete dissolution at room temperature. The resulting solution has a deep yellow color that turns to deep green after a couple of minutes. The yellow color is characteristic of V^{5+} in the form of VO_2^+. After 16 hours, the solution turned to deep blue, which is indicative of V^{4+} in the form of VO^{2+} [Kolthoff et al., 1957]. The pH of the vanadium oxalate solution was 2.1. It has been reported that solutions containing VO^{2+} are stable for months when kept in a medium or strong acid solution [Clark, 1968], and that VO^{2+} solutions were even found to be stable in air at a pH of 2.45 [Selbin, 1965]. The decrease of vanadium's valence is a result of its reduction associated with the simultaneous oxidation of oxalic acid. The proposed reactions occurring are presented below:

$$2NH_4VO_3 + [COOH]_2 \rightarrow 2[COONH_4] + 2OH^- + 2VO_2^+ \text{ (yellow)} \quad (1)$$

$$C_2O_4^{2-} \rightarrow 2e^- + 2CO_2 \quad (2)$$

$$VO_2^+ + 2H^+ + e^- \rightarrow H_2O + VO^{2+} \text{ (blue)} \quad (3)$$

The second step, which is used for the creation of aged catalysts, begins with 0.5 grams of support suspended in 50 ml of distilled water. The solution is vigorously stirred and heated to 70 °C. The volume of the aged vanadium oxalate solution (deep blue) that contains the appropriate amount of vanadium atoms that will give the desirable vanadia content on the support, is added to the above suspension. Heating and stirring is continued until most of the water evaporates and a paste is obtained. The beaker is then placed in the oven where the resulting material is dried at 125 °C for 3-4 hours. The dried powder is ground and sieved in an 80-mesh sieve.

1.2.2 Support and Catalyst Characterization

X-Ray Diffraction and BET X-ray diffraction was used to identify the phases of titania. X-ray studies were carried out on a Siemens D500 Diffractometer with a CuK_α radiation source (wavelength 1.5406 Å). Anatase and rutile phases of titania were determined from the strongest peaks corresponding to anatase ($2\theta = 25.3^\circ$ for the (101) reflection of anatase) and rutile ($2\theta = 27.5^\circ$ for the (110) reflection of rutile). The specific surface areas of the supports and catalysts were measured by nitrogen adsorption at 77 K with the BET method using a Micromeritics Gemini 2360 apparatus. All samples were dried overnight and degassed for 1.5 hr at 125 °C under helium prior to the measurement.

FT-IR Spectroscopy and NH_3-Temperature Programmed Desorption Experiments FT-IR spectroscopy was used to characterize the acidic properties of the supports and the catalysts. The experiments were performed with a Bio-Rad spectrophotometer (FTS-040). Self-supported wafers were formed by pressing 10±1 mg of material. The wafers were placed in a bakeable high-vacuum cell with CaF_2 windows and purged with pre-purified grade helium (Wright Bros. 99.995%) at 550 °C for 1 hour to remove any impurities. The sample was cooled down to 150 °C while NH_3 was introduced in the cell and continued flowing for a total of 1 hour to ensure complete saturation of the sample. Helium was then admitted to the cell at constant temperature for sufficient time to remove any physisorbed ammonia. From the recorded spectra at different desorption temperatures, conclusions about the Lewis acid sites (band at 1605 cm^{-1}) and the Brønsted acid sites (band at 1427 cm^{-1}) of the catalyst were reached.

Ammonia temperature programmed desorption experiments were carried out to ascertain the total number of acid sites on the supports and catalysts. The total acidity of the prepared and modified samples was determined with NH_3-temperature programmed desorption. 50 mg of catalyst (dry basis) was placed inside the reactor and purged with pre-purified He at 550 ^oC for 1 hour to remove any impurities. Oxygen was admitted to the bed for 1 hour to ensure that vanadium was at its fully oxidized state (V^{5+}). The sample was then loaded with ammonia for 1 hour (enough time to ensure saturation) while cooling down to 150 ^oC. The sample was kept at this temperature in helium for 6 hours to allow desorption of all physisorbed NH_3. The desorption of ammonia was achieved by heating the bed at a constant rate (6 K/min).

UV-VIS Spectrophotometer Experiments UV-VIS spectrophotometry was used to determine the valence state of vanadium in solution. Measurements were performed using a Shimadzu UV-2501PC spectrophotometer to investigate the possible valence states of vanadium ranging from V^{+2} to V^{+5}. Vanadium standards were created from vanadium chlorides (VCl_2, VCl_3, or VCl_4) or vanadium pentoxide. Since all of the vanadium compounds are highly reactive, all of the standards were prepared in a glove box under nitrogen atmosphere. The appropriate vanadium chlorides (Aldrich reagents) were dissolved in dehydrated, ethanol (Midwest Grain Products) to produce standards for V^{+2} to V^{+4}. Vanadium pentoxide (Aldrich, 99.99%) was dissolved in HCl to create the V^{+5} standard. Measuring each standard allowed the identification of significant peaks that could be used to judge the vanadium solutions used to make catalysts. More details for the wavenumbers used to characterize the various vanadium valences were given in the previous report. The features of each standard were divided into ultraviolet and visible wavelength groups.

The latter group was important, as the results for the ultraviolet wavelengths were too similar to be significant. Comparing the results obtained from the vanadium standards with two unknown solutions allowed us to determine that V^{+5} is the dominant species in the yellow vanadium precursor solution that was not aged. Similarly, we were able to show that reduced valence states of vanadium are dominant in the blue vanadium precursor solution that was allowed to age for at least 16 hours.

The results of the characterizations of the synthesized catalysts were presented in detail in the second biannual report (period of April 1, 1998 to September 30, 1998).

Catalytic Studies The catalytic experiments were conducted in a plug flow reactor under atmospheric pressure. Four anticorrosive mass flow controllers regulated the flow rates of oxygen (Wright Bros., 4.18% in He), ammonia (Matheson, 3.89% in He), nitric oxide (Air Products, 2.0% in He), and helium. The reaction mixture was fed into the reactor (1/4 in. ceramic alumina tube) through stainless steel tubing. Pre-purified grade helium (Wright Bros., 99.995%) was used as the balance gas. The inlet concentrations of NO, O_2, and NH_3 were 2000 ppm unless otherwise specified.

For the catalytic experiments, 50 mg of catalyst (dry basis) was loaded in the reactor. The tap density of the catalysts, which was measured in a graduated cylinder, used for the estimation of gas hourly space velocity was approximately 0.68 g/cm^3. The GHSV for the present study was 30,000 h^{-1} unless otherwise specified. An Omega temperature controller was used to control the furnace temperature. A type K thermocouple is inserted directly into the catalyst bed. Prior to the catalytic experiments, the catalyst was activated *in-situ* by exposing it to oxygen for 1.5 hours at 400 °C. The reactor effluent was analyzed with a thermal conductivity detector. Nitrogen and oxygen are separated with a Carboxen 1000 column (Supelco, stainless steel 1/8 in., 15 ft long, 60/80 mesh) and the nitrous oxide with a Porapak-Q column (Altech, stainless steel 1/8 in., 12 ft long, 100/120 mesh). The columns operated in parallel for the analysis of each sample at any given time on stream. In order to determine the concentration of unreacted ammonia, the effluent of the reactor passed through a solution of boric acid (0.016M) for a certain amount of time. The amount of ammonia that reacted with boric acid was determined by measuring the amount of dilute hydrochloric acid solution ($4.5*10^{-4}$ N) required to bring the pH to its initial value. Phenol Red, with a pH range of 6.6 (yellow) – 8.0 (red), was used as an indicator. The definitions of NO_X conversion and nitrogen selectivity are as follows:

$$NO_x Conversion = \frac{(NO_{in} - NO_{x,out})}{NO_{in}} \times 100 \qquad \text{(I)}$$

$$N_2 Selectivity = \frac{N_2}{(N_2 + N_2O)} \times 100 \qquad \text{(II)}$$

The moles of NO_x (including NO and NO_2) in the reactor effluent can be determined from the following atomic nitrogen balance:

$$NO_{x,out} = NO_{in} + NH_{3,in} - 2(N_{2,out}) - 2(N_2O_{out}) - NH_{3,out} \qquad \text{(III)}$$

1.3 RESULTS AND DISCUSSION

The purpose of this document is to present the catalytic behavior of selected mixed oxide supports loaded with vanadia for the selective catalytic reduction of NO. The comparison was performed under similar operating conditions, while the vanadium was loaded on the support following two variations of wet impregnation. Catalysts were made with and without aging of the precursor solution before its addition to the support. As it will be shown below, the vanadium impregnation method is crucial to catalyst performance. The materials prepared in the present study exhibited a wide range of BET surface areas. The values obtained for several supports at different calcination temperatures are presented in Table 2.

Table 2. *BET areas of the supports used in the present study*

Calcination T	P25	TiO_2/WO_3	TiO_2/ZrO_2	TiO_2/Cr_2O_3	$TiO_2/SiO_2/Al_2O_3$
400 ^oC	61 m^2/g	164 m^2/g	217 m^2/g	65 m^2/g	126 m^2/g
500 ^oC	57 m^2/g	131 m^2/g	87 m^2/g	28 m^2/g	96 m^2/g
600 ^oC	57 m^2/g	74 m^2/g	69 m^2/g	21 m^2/g	80 m^2/g
700 ^oC		36 m^2/g			

The BET area of P25 titania was also measured for comparison. The TiO_2/Cr_2O_3 composite possesses a lower BET area than one would expect, since amorphous chromia was reported to have areas as high as 200 m^2/g [Curry-Hyde and Baiker, 1985]. The rest of the polyoxides synthesized in this work have relatively high surface areas. It should be noted that in contrast to the commercial sample (Degussa P25), the surface area of the synthesized supports decreases rapidly with an increase in calcination temperature.

In all cases there is a loss of BET area after impregnation with V_2O_5, which is more pronounced for the high surface area supports. Other researchers [Amiridis et al., 1994; Went et al., 1992a] found a similar trend showing that the BET area of vanadia $DeNO_x$ catalysts decreased as the weight percent of vanadia increased. Others [Lietti et al., 1996] also reported a decrease in the surface area of TiO_2/WO_3 supports after impregnation with vanadia; however, it was for smaller vanadia contents of 1.47 % w/w. The XRD analysis of the supports revealed that with the exception of the titania phase of the oxide supports (the primary component of the composite oxides), only tungsten acquires some form of crystallinity (Figure 1). However, it was found that TiO_2/WO_3, after calcination at 700 ^oC, does acquire crystalline WO_3 (not shown). The same

material, when calcined at 500 ^{o}C, has anatase titania as its only crystalline phase. These results are in close agreement with [Cristiani et al., 1993], who reported only anatase titania for TiO_2/WO_3 composites calcined up to 800 ^{o}C and crystalline WO_3 at temperatures higher than 800 ^{o}C.

The XRD spectrum of P25 was included for comparison. In the case of a fully crystalline material such as P25 titania, we were able to confirm the manufacturer's specification, which indicated 85% anatase and 15% rutile titania content, within 1% accuracy using the Spurr–Myers equation [Spurr and Myers, 1957]. This correlation is for pure titanias; therefore, it cannot be used for quantitative determination of the anatase and rutile phases of the polyoxide supports because of the coexistence of one or more additional oxides. The titania component of the oxide supports we synthesized was not completely crystalline, and the addition of other oxides altered the phases of titania. As shown in Figure 1, the incorporation of W or Zr results in the formation of only anatase (peak at $2\theta=25.3^{o}$). No rutile peak ($2\theta=27.5^{o}$) was observed for either support. The crystallinity of Cr_2O_3/TiO_2 is low, and titania is in the form of rutile. Similarly, low titania crystallinity is observed for the support containing Al and Si. In contrast to the previous support, the incorporation of Al and Si leads to the formation of anatase titania. It is worth noting that the XRD spectra of vanadia loaded supports did not show any crystalline vanadia, even at the highest loading (V_2O_5 10 wt %) employed in this work.

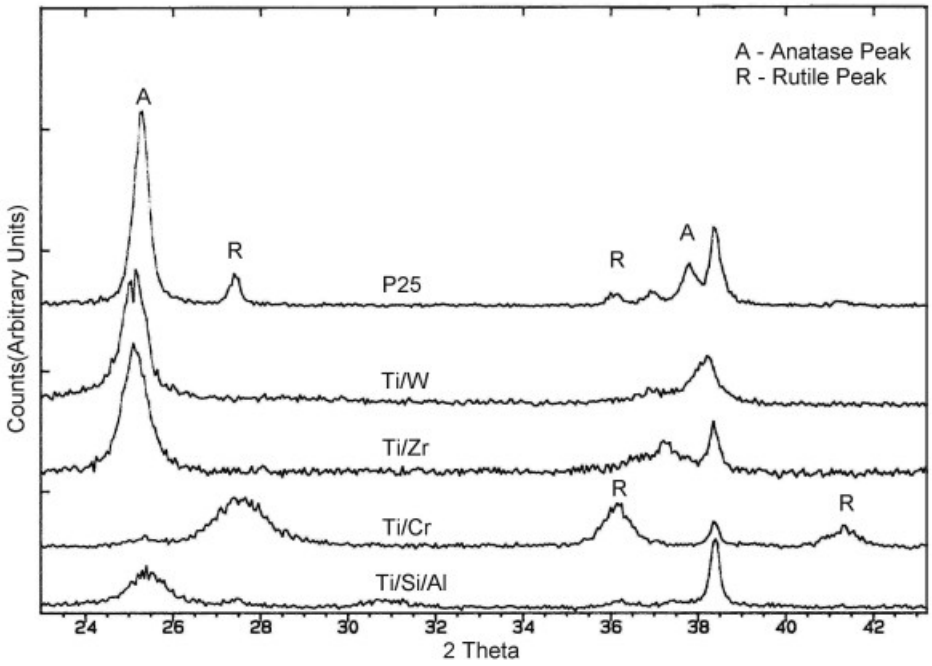

Figure 1. *XRD patterns of several TiO_2-based suports. The atomic ratios of the metals are Ti/W=30/5, Ti/Zr=30/5, Ti/Cr=30/5, and Ti/Si/Al=30/2/1.*

The oxidation conditions for the preparation of these samples were identical with those used during the *in-situ* activation of the catalyst prior to reaction. This indicates that vanadia is probably well dispersed on the support. Several researchers [Amiridis et al., 1994; Went et al., 1992a; Lietti et al., 1996] found with Raman-IR that increasing the vanadia loading alters the relative population of the monomeric vanadia species (band at ~ 1030 cm^{-1}) and polymeric vanadia species (band at ~ 930 cm^{-1}). It was found that vanadia loadings above that corresponding to monolayer coverage result in the formation of V_2O_5 crystallites at the expense of other vanadia species. The supports synthesized in this study (Table 2) were loaded with V_2O_5 and tested for effectiveness under identical conditions. Prior to vanadia impregnation, the supports were calcined at 500 ^oC for 3 hours unless otherwise specified.

It is worth noting that the specific methodology of adding the vanadia precursor is essential for the development of efficient catalysts. As mentioned earlier in this paper, we utilized wet impregnation for the loading of vanadium. Two variations of the method were followed, which were based on: 1) the direct addition of individual solutions to the suspension containing the support and 2) aging the vanadium precursor solution before addition to the support. These two variations of the impregnation technique result in different vanadium valence states in the precursor solution during the impregnation step. More specifically, the first one results in V^{5+} while the second one (aging of the precursor solution) results in V^{4+}. The vanadium standards, which were created to identify unknown vanadium valence states, revealed valuable distinguishing characteristics for each valence state. Once the standards were characterized, the valence state of the aged blue vanadium solution used on the supports could be determined. The UV-vis results suggest the presence of V^{+4} and other reduced valence states in the aged vanadium solution.

Surprisingly, this difference in vanadium valence during impregnation has a tremendous effect on the catalytic performance of the catalysts tested under identical activation and operating conditions. We present in Table 3 the catalytic behavior of WO_3/TiO_2 + 5wt% V_2O_5 and P25 + 6.4wt% V_2O_5, which were prepared with and without aging of the vanadium precursors. The catalysts were tested at 400 ^oC with the same feed composition. It is remarkable to observe that the catalysts synthesized with the aged vanadium precursor solution resulted in significantly better performance than those made without aging the precursor. This trend was consistent for temperatures varying from 200 ^oC to 400 ^oC. Our results indicate that even if the catalysts undergo the same activation conditions (oxidation for the transformation of vanadium to V_2O_5), the valence of vanadium during the initial stages of the impregnation step plays a very important role on its catalytic performance. Perhaps V^{+5} does not bond to the support as readily as V^{+4}, which could lead to orientations of vanadium pentoxide that contain obstructed centers. In addition, the relative concentrations of polymeric and monomeric vanadium species may be quite different, which could affect catalytic performance. Even at temperatures up to 400 ^oC, nitrogen selectivity and NO conversion remain high for WO_3/TiO_2 impregnated with the aged vanadium solution. The XRD analyses of the catalysts synthesized with both variations of the impregnation step did not show any peaks corresponding to crystalline vanadia, thus indicating that vanadia is well dispersed regardless of the loading method. This was expected because the interaction between crystalline titania and vanadia is strong and usually results in high vanadia dispersion [Went et al., 1990; Roozeboom et al., 1980]. The above data indicate that aging the precursor

solution, which is associated with the formation of V^{4+}, can result in effective vanadia-based catalysts.

Table 3. *NO conversion and N_2 selectivity over P25 and WO_3/TiO_2 (W/Ti=5/30) at 400 ^oC loaded with vanadia with and without aging of the vanadium precursor. The catalysts were activated at 400 ^oC for 1.5 hours in oxygen (GHSV=30,000 h^{-1}, NO=2000 ppm, NH_3=2000 ppm, O_2=2000 ppm, time on stream = 2 hours).*

	P25 (6.4wt % V_2O_5)		WO_3/TiO_2 (5wt % V_2O_5)	
	without aging	with aging	without aging	with aging
NO Conversion	28 %	89 %	73 %	100 %
N_2 Selectivity	43 %	56 %	89 %	90 %

1.3.1 Comparison of the Catalysts Synthesized

The screening for effectiveness of supports loaded with comparable amounts of vanadia was performed under identical operating conditions to identify the most promising catalysts for the SCR of NO. The results of this screening are presented in Figure 2 at 300 ^oC when equimolar amounts of NO, O_2, and NH_3 are added into the reactor. All the catalysts presented in this figure, if not otherwise specified, were synthesized with the aged vanadium solution. One can observe that WO_3/TiO_2 with 5 wt % V_2O_5 demonstrated exceptional behavior since both the NO conversion and selectivity to nitrogen were 100 %. The atomic ratio of metals in this support was Ti/W=30/5, which corresponds to 33 wt % WO_3. This concentration of tungsten is significantly higher than that used in industry [Ramis et al., 1992]. When the relative concentration of W on the support decreases to 5 wt% WO_3, which corresponds to Ti/W=30/0.5, both the NO conversion and the N_2 selectivity decrease to about 95 % (Figure 2). The concentration of tungsten on the latter support is comparable with that used in industry [Ramis et al., 1992]. Evidently, this change of performance is attributed to the decrease in tungsten concentration. Our infrared investigations showed that for catalysts with the same vanadia loading, a decrease in the tungsten concentration results in a significant decrease in the number of Brønsted acid sites on the catalyst. When P25 titania was used as the support (P25+6.4 %V), the performance of the catalyst was comparable to that of WO_3/TiO_2-based catalysts. Specifically, the NO conversion and N_2 selectivity are in the vicinity of 97 %. The vanadia loading for these catalysts is below that theoretically required for monolayer coverage based on the BET surface area of the supports. It was proposed [Bond and Brückman, 1981; Bond and Tahir, 1991] that in order to achieve a monolayer of vanadia on titania, 0.145 wt % V_2O_5/m^2 of support should be added.

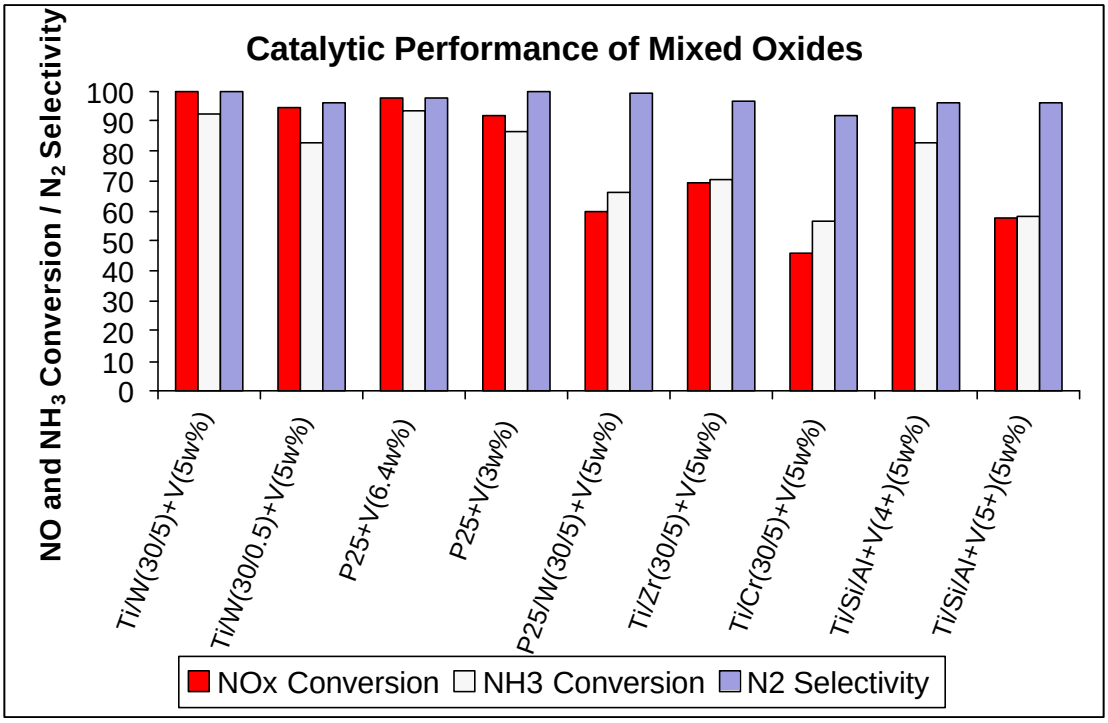

Figure 2. *NO conversion, NH_3 conversion and N_2 selectivity of selected catalysts at 300 ^oC (GHSV=30,000 h^{-1}, NO=2000 ppm, NH_3=2000 ppm, O_2=2000 ppm, time on stream 2 hours). All supports were calcined at 500 ^oC and oxidized for 1.5 hours at 450 ^oC. The aged vanadium oxalate solution was used for all catalysts with the exception of Ti/Si/Al+V(5+)(5w%).*

It is worth noting that even though the vanadia loading of P25 is higher than that of the Ti/W+5%V catalyst, the performance of the latter catalyst is better (100% NO conversion and 100% N_2 selectivity) than that of the P25-based catalysts. It is well demonstrated [Topsøe, 1994; Topsøe et al., 1995a; Topsøe et al., 1995b] that the Brønsted acid sites associated with V^{5+}-OH and the redox sites (V^{5+}=O) are responsible for the SCR activity. Hence, one would expect that P25+6.4%V will be more active than Ti/W+5%V due to the difference in vanadia loading. However, the activity of the tungsten-doped catalysts can be explained by the acidic properties of the catalysts. The ammonia TPD experiments we performed (not shown) demonstrated that the W-based catalysts have significantly more acid sites than P25 for comparable levels of vanadia loading. Moreover, the shape of the ammonia desorption peak for the WO_3/TiO_2-based catalysts was shifted towards higher temperatures, thus indicating that the associated acid sites are of higher strength. Other researchers [Lietti et al., 1993] also found that the acid sites of WO_3/TiO_2 are stronger than those of V_2O_5-TiO_2. It was also concluded that the ternary oxides (W, V, Ti) are more active than any combination of the binary ones due to strong electrostatic interactions involving these three oxides [Alemani et al., 1995].

At this point the stepwise temperature programmed desorption (STPD) experiments should be explained in greater detail. This method has been used very successfully [Robb et al., 1998] to characterize zeolites and gave distinct desorption peaks which correspond to either Lewis or Brønsted acid sites when the temperature increases. This information was obtained by performing

a simulated STPD experiment in the cell. Our work with the present $DeNO_x$ catalysts proves that there are not distinct temperature limits for the strength of both Lewis and Brønsted sites. The FT-IR spectra of the $V_2O_5/WO_3/TiO_2$ catalysts show the existence of a major Brønsted peak at 1427 cm^{-1} (asymmetric deformation of NH_4^+) and peaks corresponding to Lewis sites at 1604 cm^{-1} (asymmetric deformation of coordinated ammonia). One can also observe a broad peak near 1660 cm^{-1}, which corresponds to W-OH Brønsted acid sites [Lietti et al., 1993]. FT-IR investigations indicated that the WO_3/TiO_2-based catalysts possess a higher number of Brønsted to Lewis sites than the P25 catalyst for comparable vanadia loading. It seems likely that the existence of additional Brønsted sites on the support probably favors NH_3 adsorption on the surface. The increased adsorption of NH_3 on the surface then increases the number of NO molecules that are adjacent to the reductant. When the vanadia content on P25 decreases, the catalyst activity decreases as expected (P25+3%V).

The incorporation of tungsten during the synthesis of the support improves catalytic performance. Others [Ramis et al., 1992] found that the incorporation of tungsten oxide not only improves the thermal stability and the acidic properties of the catalyst but also retards the transformation of anatase to rutile. A composite oxide support containing WO_3 and P25 titania was synthesized by modifying the sol gel technique described earlier using the same atomic ratio of metals (Ti/W=30/5). The tungsten precursor was mixed with the appropriate concentration of a suspension containing P25 titania. The resulting support (P25/W) was treated under identical conditions with the previous catalysts and loaded with vanadia. The catalytic results with these catalysts are presented in Figure 2. One can observe that even though P25 is very selective in transforming NO to N_2, its activity remains at low levels. We believe that the low reactivity observed is a result of the low extent of mixing between the two oxides of the support, which probably results in "islands" of WO_3 deposited on P25.

The effect of dopants such as Zr and Cr on titania was investigated as well. These supports (Ti/Me=30/5, where Me stands for Zr or Cr) were loaded with 5 wt % V_2O_5 and catalytically tested under identical conditions. It was shown (Figure 2) that these catalysts performed very poorly. This behavior is consistent with the acidity characteristics of the catalysts. The ZrO_2/TiO_2 supports acquired only a small number of Lewis acid sites. Others [Tanabe et al., 1989] also mentioned that the combination of either Zr or Cr with Ti does not lead to strong acidity unless one adds SO_4^{-2} anions. The FT-IR investigations showed that the zirconium-based catalysts possessed a relatively small number of Brønsted and Lewis acid sites. Evidently, loading the supports with vanadia is responsible for the generation of Brønsted sites (Table 4). Very similar catalytic behavior was observed when chromium was the dopant for TiO_2. The SCR activity was the lowest observed among all the catalysts tested in the present study. This is consistent with the FT-IR studies, which indicate that the number of Brønsted sites on the Cr doped catalysts is practically negligible. The catalyst possesses only Lewis sites.

Table 4. *Ratios of the areas of Brønsted to Lewis peaks (B/L) for the catalysts involved in the present study after they were treated with ammonia (the ratios were formed from the bands at 1427 and 1604 cm^{-1}, respectively). The wafers were heated at 150 ^{o}C.*

WO_3/TiO_2 B/L=0.98	WO_3/TiO_2(2 wt% V_2O_5) B/L=1.85	WO_3/TiO_2(5 wt% V_2O_5) B/L=5.56	WO_3/TiO_2(10 wt% V_2O_5) B/L=6.67
P25 only Lewis sites	P25 (3 wt% V_2O_5) B/L=1.82	P25(6.4 wt% V_2O_5) B/L=4.54	P25(10 wt% V_2O_5) B/L=5.88
ZrO_2/TiO_2 B/L=0.08	ZrO_2/TiO_2(5 wt% V_2O_5) B/L=4.17	Cr_2O_3/TiO_2(5 wt% V_2O_5) B/L=0.06	WO_3/TiO_2(5 wt% V_2O_5) B/L=4.76

The performance of the ternary oxide (Ti/Si/Al=30/2/1) loaded with 5 wt % V_2O_5 was also tested. As mentioned earlier, vanadia was loaded after aging the precursor solution. The amount of vanadia present was below that stoichiometrically required for monolayer coverage. Our catalytic results show that this catalyst is as effective as the most efficient catalyst identified in this study, which was based on tungsten doped titania (Ti/W+5%V). More specifically, under identical operating conditions with those used to test the other catalysts, this catalyst completely converted the nitric oxide and nitrogen selectivity was more than 98%. The FT-IR experiments indicate that the catalyst possesses a large number of Brønsted acid sites, which are almost comparable with those of the tungsten doped titania catalyst. The enhanced Brønsted acidity is a result of both the vanadia (V^{5+}-OH) added and the support. In contrast to pure titania, which contains Lewis acid sites exclusively [Morterra et al., 1980], the incorporation of either Si or Al can result in a major increase in Brønsted acid sites. The XRD spectrum of $Al_2O_3/SiO_2/TiO_2$ showed only a short peak assigned to anatase (Figure 1).

Earlier in this report it was mentioned that crystalline titania significantly favors the dispersion of vanadia species and consequently the SCR performance. Previous studies [Handy et al., 1992; Amiridis et al., 1994] demonstrated that highly crystalline titania is required for the synthesis of effective DeNOx catalysts because it favors the dispersion of vanadia. The Spurr-Myers correlation cannot be applied to provide quantitative information for this support since it was developed for pure titanias. However, a simple comparison of this spectrum with that of P25 indicates that the crystallinity of the ternary oxide support used for the synthesis of this catalyst was very low. It is remarkable to note that the present catalyst demonstrates exceptional DeNOx behavior even though the crystallinity of the support is low; this catalyst was loaded with vanadia using an aged vanadium oxalate solution. The same support, loaded with the same amount of vanadia but created without aging the vanadium precursor solution (NH_4VO_3 and oxalic acid), gave significantly lower activity and N_2 selectivity (Figure 2) under identical activation and operation conditions. The catalytic behavior of this material is consistent with our earlier work [Economidis et al., 1998] involving Si and Al doped titanias loaded with vanadia. This observation indicates that aging the vanadia precursor solution during the impregnation step, which is associated with the formation of V^{4+} species in the precursor solution, is crucial for the synthesis of high performance DeNOx catalysts.

1.3.2 Performance of WO_3/TiO_2-based catalysts versus temperature

It was found under identical operating conditions that the WO_3/TiO_2 support loaded with vanadia was the most effective catalyst. It was followed by V_2O_5-P25 and V_2O_5-$Al_2O_3/SiO_2/TiO_2$. The performance of this catalyst (Ti/W+5%V) with different loadings of vanadia as a function of the reaction temperature in the range of 200 - 400 ^oC is presented in Figures 3 and 4. The NO conversion increases abruptly with temperature and finally reaches a plateau value. For vanadia loadings higher than 5 wt %, the NO conversion becomes complete at 250 ^oC and remains at this level for temperatures higher than 400 ^oC. For lower vanadia loadings the conversion reaches a plateau at higher temperatures (about 300 ^oC). The ammonia conversion (not shown) closely follows the trend of NO conversion for all three catalysts presented in Figure 3 at any temperature. According to the redox cycle proposed by others [Topsøe 1994; Topsøe et al., 1995a], the reduction of one NO molecule to N_2 requires one ammonia molecule. This behavior indicates that this catalyst effectively utilizes ammonia over a wide range of temperatures. This was not the case in our earlier work performed under identical operating conditions [Economidis et al., 1998]. In that work titania-based catalysts loaded with the same amount of vanadia without aging were found to oxidize ammonia. As a result, poor $DeNO_x$ activity was observed.

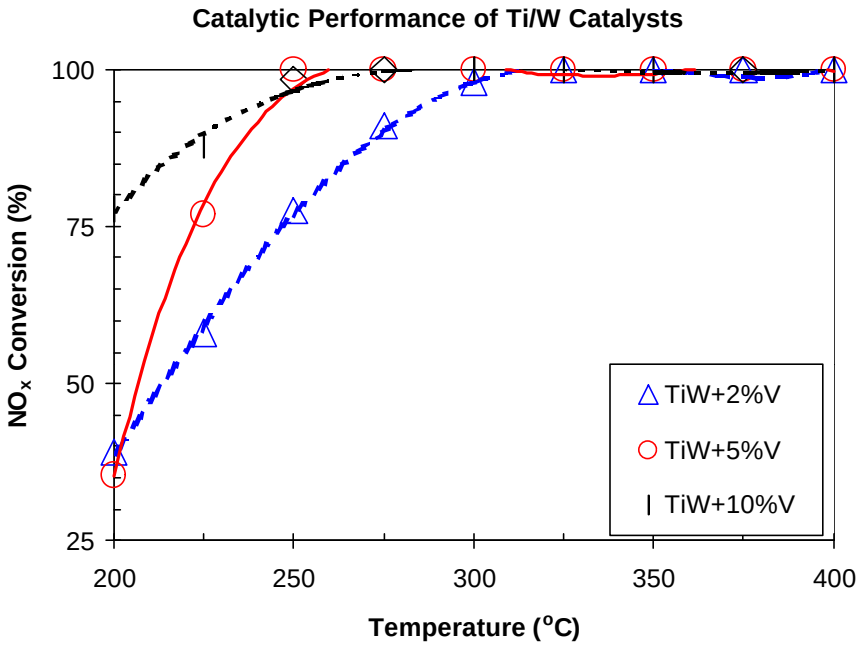

Figure 3. *NO conversion versus the reaction temperature over WO_3/TiO_2 (W/Ti=5/30) loaded with different amounts of V_2O_5 (GHSV=30,000 h^{-1}, NO=2000 ppm, NH_3=2000 ppm, O_2=2000 ppm, time on stream 2 hours).*

The WO_3/TiO_2 catalyst gave high values for N_2 selectivity (Figure 4) over a wide temperature range. When the loading of vanadia is 2 and 5 wt%, the nitrogen selectivity remains higher than 97% for temperatures as high as 375 ^oC before dropping. By combining this information with the activity characteristics of the catalyst presented in Figure 3, one can conclude that the catalyst with 5 wt% V_2O_5 indeed exhibits superior performance. More specifically, NO is transformed to N_2 with yields higher than 97 % in the range of 250 ^oC to 375 ^oC.

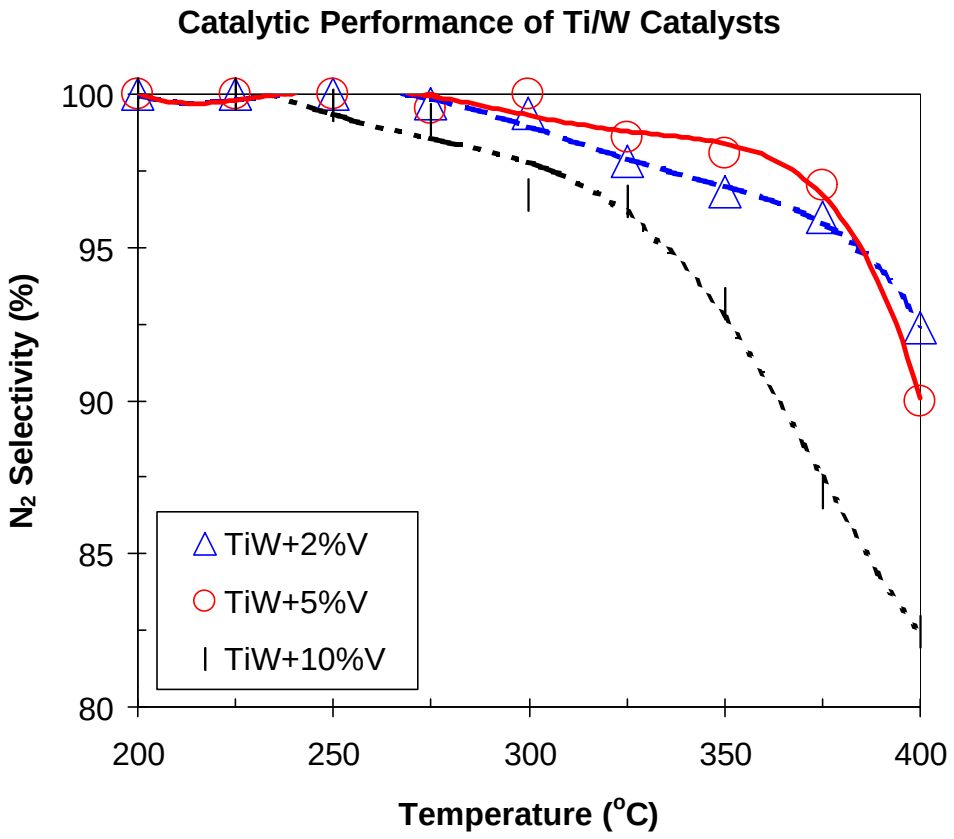

Figure 4. *N_2 selectivity versus the reaction temperature over WO_3/TiO_2 (W/Ti=5/30) loaded with different amounts of V_2O_5 (GHSV=30,000 h^{-1}, NO=2000 ppm, NH_3=2000 ppm, O_2=2000 ppm, time on stream=2 hours).*

For higher temperatures the nitrous oxide selectivity increases at the expense of nitrogen selectivity. The catalyst is not very active at low temperatures for lower vanadia loadings, while the N_2 selectivity decreases for high vanadia content catalysts (10 wt %). This is most noticeable at relatively high temperatures. This behavior at intermediate levels of vanadia loading (5 wt%) is probably associated with the maximum in the concentration of acid sites as probed by the NH_3-TPD experiments. Other researchers observed a decrease in N_2 selectivity at relatively high vanadia concentrations that approached the theoretical monolayer [Went et al., 1992a]. This behavior was associated with the increase in concentration of vanadia crystallites.

The performance of P25 titania loaded with vanadia as a function of temperature is presented in figures 5 and 6.

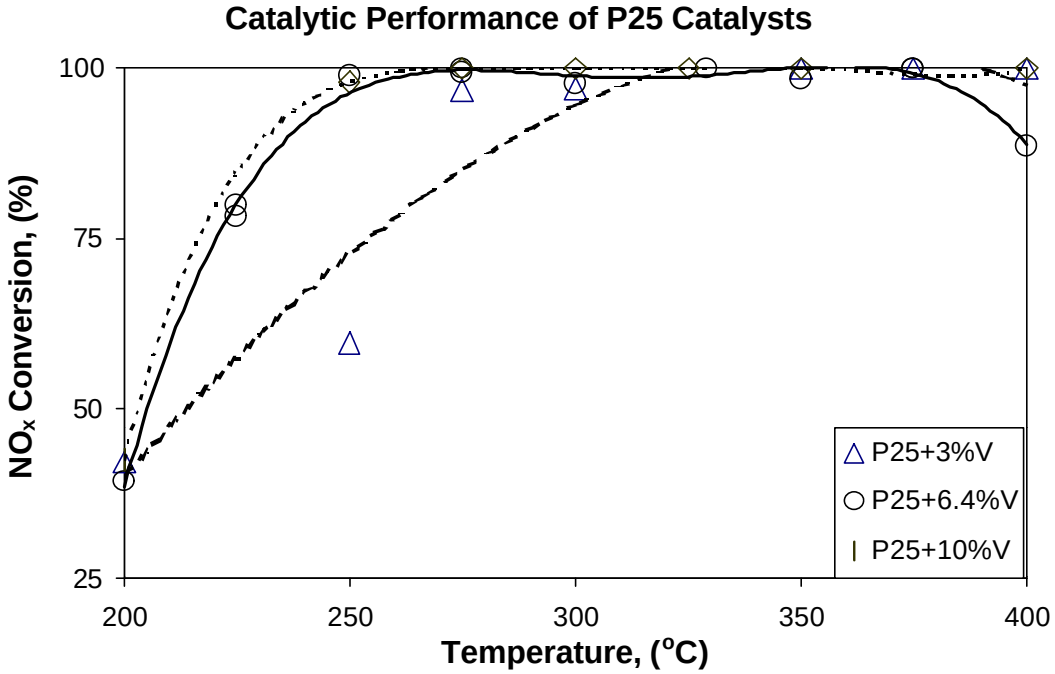

Figure 5. *NO conversion versus the reaction temperature over P25 loaded with different amounts of V_2O_5 (GHSV=30,000 h^{-1}, NO=2000 ppm, NH_3=2000 ppm, O_2=2000 ppm, time on stream=2 hours).*

Similar trends with the case of W/TiO_2 catalysts loaded with vanadia are observed. More specifically, the NO conversion increases with temperature and reaches about 100% at temperatures higher than about 275 ^oC. This temperature is slightly higher than the case of W/TiO_2-based catalysts. The increase of the vanadia content above 3 wt% improves dramatically the NO conversion at lower temperatures. At low temperatures NO is transformed completely to nitrogen (figure 6) while for temperatures higher than about 275 ^oC N_2O evolves. The selectivity of nitrogen decreases rapidly with temperature.

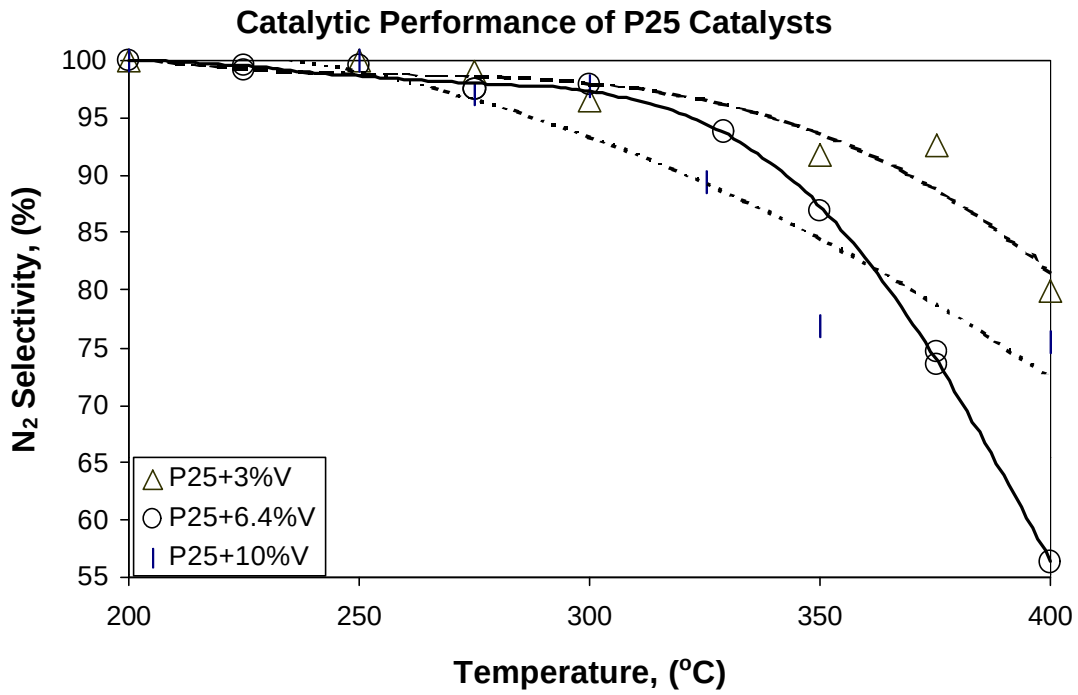

Figure 6. *N_2 selectivity versus the reaction temperature over P25 loaded with different amounts of V_2O_5 (GHSV=30,000 h^{-1}, NO=2000 ppm, NH_3=2000 ppm, O_2=2000 ppm, time on stream=2 hours).*

A comparison between the W/TiO_2- and P25-based catalysts shows that for comparable vanadia loadings the former catalysts exhibit (compare Figures 4 with 6, respectively) significantly higher nitrogen selectivities for the same temperature (Economidis et al., 1999). This behavior shows that the former group of catalysts is significantly better since it offers a wider temperature window for optimum operation.

1.4 CONCLUSIONS

Several TiO_2-based catalysts were tested with synthetic flue gas. It was found that the valence of vanadium in the precursor solution during the wet impregnation synthesis of TiO_2-based SCR catalysts plays a very important role. More specifically, the reduction of V^{5+} to V^{4+} with the simultaneous oxidation of oxalic acid after the solution is aged results in better catalysts. It is worth noting that a vanadium precursor solution containing V^{4+}, if added to highly acidic titania-based supports with low crystallinity, leads to enhanced performance. This does not normally lead to effective SCR catalysts. It was concluded that among W, Zr, Cr, Al, and Si doped titanias, WO_3/TiO_2 supports with relatively high concentrations of tungsten form the most active and N_2 selective catalysts. Moreover, these catalysts had the widest temperature window for optimum operation.

II. SURFACE CHARACTERIZATION OF CATALYSTS SYNTHESIZED FROM V^{4+} OR V^{5+}

ABSTRACT

A number of characterization techniques have been employed to study the characteristics of titania-supported vanadium pentoxide catalysts for the selective catalytic reduction of nitric oxide. Earlier results had showed a difference in catalytic performance as a function of vanadium valence state in the vanadium precursor solution. A number of catalysts on different types of titania supports were synthesized from V^{+4} and V^{+5} solutions. The relationship between changes in catalytic performance for similar catalysts synthesized with V^{+4} vs. V^{+5} is more complex than what was originally observed. Surprisingly, X-ray photoelectron spectroscopy results for uncalcined catalysts actually revealed that the surface vanadium species for catalysts synthesized from the V^{+4} solution behave more like V^{+5} than those species deposited from the V^{+5} solution. Oxygen chemisorption experiments did not reveal any significant differences in the vanadium valence state used during synthesis and metal dispersion. UV-VIS spectroscopy, capillary electrophoresis, and capillary electrophoresis combined with inductively coupled plasma mass spectroscopy were used in an attempt to quantitatively determine the distribution of vanadium valence states in the aged vanadium oxalate solution. The complexity of the vanadium oxalate solution only allowed qualitative observations to be made. A potentiometric titration method is currently being developed to measure the relative quantities of V^{+3}, V^{+4}, and V^{+5} in the vanadium oxalate solution.

INTRODUCTION

This section covers the second phase of this project. The work performed during this phase focused on the selective catalytic reduction of NO_x. The work primarily aimed at understanding the catalytic differences observed in catalysts synthesized from V^{+4} and V^{+5} solutions. The catalysts synthesized from V^{+4} were made from a modified vanadia loading procedure developed in our laboratories for the synthesis of TiO_2-based catalysts. A set of catalysts was synthesized to particularly study the effects of different vanadium valence states on TiO_2 supports with different properties. A number of characterization techniques were employed to study the surface characteristics of the catalysts and the properties of the vanadium precursor solution. Understanding vanadium's role during synthesis could lead to the successful manipulation of synthesis parameters to create materials with the catalytic properties necessary for our reaction system.

2.1 EXPERIMENTAL WORK

2.2.1 Catalyst Preparation

The titania-supported catalysts described here were prepared by two different wet impregnation methods (Economidis et al., 1999). The first method is believed to add vanadium to the support in the V^{+5} valence state. The second method, which utilizes the aged vanadium oxalate solution, is believed to add vanadium to the support in the V^{+4} valence state. Both methods heat the slurry until a thick paste is formed. The catalysts are then dried at 110°C, ground with a mortar and pestle, and sieved through an 80 mesh screen. Finally, the catalysts are calcined at 400-500°C under a flow of 4% oxygen in helium.

Figure 7 illustrates how catalysts were synthesized with multiple valence states of vanadium. First, the required amount of vanadium precursor that would yield approximately 10% of theoretical monolayer coverage was added to the support in the same manner as described above. Second, the catalyst would be dried at 110°C, ground, and sieved through an 80 mesh screen. Third, the vanadium addition procedure would be repeated so that the final catalyst would be covered with enough vanadium to yield theoretical monolayer coverage. Fourth, this final slurry would be dried at 110°C, ground, and sieved through an 80 mesh screen. Calcination of the catalyst would be the next step before catalytic tests.

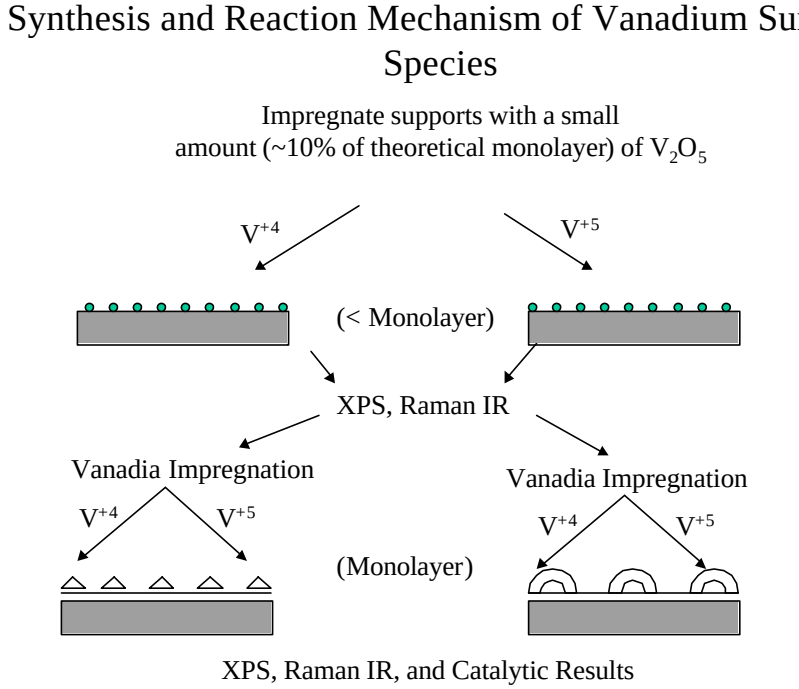

Figure 7. *Sequenced synthesis of V_2O_5/TiO_2 catalysts*

2.2.2 Characterization

Chemisorption Chemisorption experiments were performed on a Micromeritics ASAP 2010C chemisorption unit. All gases used are of ultra-high purity (99.98%), and all samples were degassed at 140°C at atmospheric pressure prior to analysis. Oxygen chemisorption at 370°C was carried out to determine metal dispersion values.

XPS X-ray photoelectron spectroscopy was used to analyze concentration of vanadium on the surface of the catalyst. The spectra were recorded with a Perkin-Elmer Model 5300 X-ray photoelectron spectrometer using $MgK_{á}$ (1253.6 eV) as a radiation source at 300 Watts. The spectra were recorded in the fixed analyzer transmission mode with pass energies of 89.45 and 35.75 eV for recording survey and high resolution spectra, respectively. The catalysts were mounted on a sample holder and degassed overnight at room temperature at 10^{-7} Torr. Correcting the observed spectra for Ti $2p_{3/2}$ binding energy of 458.5 eV eliminated sample-charging effects. The spectra were smoothened and a nonlinear background was subtracted. Deconvolution was performed using Gaussian and Lorenzian curves.

XRD X-ray diffraction was used to identify the phases of titania. X-ray studies were carried out on a Siemens D500 Diffractometer with a CuK_{α} radiation source (wavelength 1.5406 Å). Anatase and rutile phases of titania were determined from the strongest peaks corresponding to anatase (2θ = 25.3° for the (101) reflection of anatase) and rutile (2θ = 27.5° for the (110) reflection of rutile).

2.2.3 Quantitative Vanadium Precursor Solution Analysis

UV/Vis (Ultra Violet/Visible Spectroscopy), CE (Capillary Electrophoresis), CE-ICP/MS (Capillary Electrophoresis-Inductively Coupled Plasma/Mass Spectroscopy), and Potentiometric Titrations All of the samples used to study the distribution of vanadium valence states in aqueous solution consisted of the aged vanadium oxalate solution itself or aqueous solutions of ammonium metavanadate or vanadyl sulfate hydrate. The only deviation to this method was during the potentiometric titrations. This method (Wang and Barteau, 2000) involved diluting the aged vanadium oxalate solution in 2M H_2SO_4 before proceeding with the analysis. The first step of the titration was the addition of 0.01N $KMnO_4$, which oxidized all of the vanadium species to V^{+5}. After adding sodium diphenylamine-4-sulfate as an indicator to the previous solution, 0.01 N ammonium iron (II) sulfate was added. Finally, another sample of the original aged vanadium oxalate solution that had been diluted in 2M H_2SO_4 was then titrated with 0.01 N ammonium iron (II) sulfate solution. The distribution of vanadium valence states could then be calculated from the volumes of the titrants added above.

2.2.4 Catalytic Studies

The catalytic experiments were conducted in a plug flow differential reactor under atmospheric pressure. Four anticorrosive mass flow controllers regulated the flow rates of oxygen (Wright Bros., 4.18% in He), ammonia (Matheson, 3.89% in He), nitric oxide (Air Products, 2.0% in He), and helium. The reaction mixture was fed into the reactor (1/4 in. ceramic alumina tube) through stainless steel tubing. Pre-purified grade helium (Wright Bros., 99.995%) was used as the balance gas. The inlet concentrations of NO, O_2, and NH_3 were 2000 ppm unless otherwise specified. 100 mg of catalyst (dry basis) was loaded in the reactor. The tap density of the catalysts, which was measured in a graduated cylinder, used for the estimation of gas hourly space velocity was approximately 0.68 g/cm^3. The gas hourly space velocity (GHSV) for the present study was 50,000 h^{-1} unless otherwise specified. An Omega temperature controller was used to control the furnace temperature. A type K thermocouple is inserted directly into the catalyst bed. Prior to the catalytic experiments, the catalyst was activated *in-situ* by exposing it to oxygen for 1.5 hours at 400 °C. The reactor effluent was continuously monitored using a MKS PPT Residual Gas Analyzer Quadrupole Mass Spectrometer.

2.2 RESULTS AND DISCUSSION

With the aim of understanding the different catalytic performance observed in V_2O_5/TiO_2 catalysts prepared from V^{+4} or V^{+5} solutions, a number of catalysts supported on different titania supports were synthesized and tested. The physical characteristics of the supports used are shown in Table 5. Hombikat and Aldrich have the highest and lowest surface areas, respectively; the other 3 supports have approximately the same area, with Ishihara having slightly more area.

Table 5. *Physical characteristics of the different supports*

Support	XRD phase	S.S.A.	Pore volume	P.D.
		(m^2/g)	(cm^3/g)	(nm)
Hombikat TiO_2	Anatase	309	0.366	4.5
Ishihara TiO_2	Anatase	63	0.340	37.8
Aldrich TiO_2	Anatase	9	0.029	13.1
Kemira TiO_2	Rutile	52	0.220	16.7
P25 TiO_2	A:R (80:20)	51	0.182	14.8

n.d.: not determined, A: anatase, R: rutile, P.D.: Pore diameter

Table 6. *Composition, metal dispersion, and percentage of mass loss upon calcination for catalysts used in this study for different levels of monolayer coverage and vanadium valence state.*

TiO_2 Support	V_2O_5 (wt%)	# Theoretical Monolayers	V^{+4} Solution		V^{+5} Solution	
			Dispersion (%)	Calcination Mass Loss (%)	Dispersion (%)	Calcination Mass Loss (%)
Hombikat	22.4	1	30	27	29	31.3
Ishihara	4.6	1	57	5.6	55	3.6
Kemira	3.8	1	36	11.7	n.d.	8.2
Degussa P25	3.7	1	n.d.	5.6	38	6.5
Aldrich	0.7	1	38	1.6	29	2
Hombikat	44.8	2	24	27.1	n.d.	n.d.
Ishihara	9.1	2	55	8.6	n.d.	n.d.
Kemira	7.5	2	31	18	n.d.	n.d.
Degussa P25	7.4	2	44	9.2	n.d.	n.d.
Aldrich	1.3	2	47	4	n.d.	n.d.
Hombikat	10	0.5	52	19.7	48	15.7
Ishihara	10	2.2	38	4	n.d.	4
Kemira	10	2.7	29	20.3	29	21.8
Degussa P25	10	2.7	38	16.9	37	12.1
Aldrich	10	15.3	15	14.7	19	8.8

Table 6 shows the metal dispersion values for the catalysts studied. Looking at the bottom 1/3 of the table shows that there is not a significant difference in metal dispersion values for the catalysts discussed above. The low dispersion values for Aldrich are expected, since it has the lowest surface area of all the supports (Table 1). Examining the other 4 titania supports in this category reveals that metal dispersion is not a strong function of vanadium valence state in the precursor solution. The dispersion values for the supports with intermediate surface area values also have intermediate dispersion values relative to Aldrich and Hombikat TiO_2. Coincidentally Hombikat TiO_2, which has the highest surface area and dispersion, also has a 4% difference in metal dispersion. This is comparable to the 4% difference in metal dispersion for Aldrich TiO_2. All of this information strongly suggests that the difference in catalytic performance for different vanadium valence states during synthesis cannot be attributed to differences in active metal dispersion. Similarly, no trends are observed in the percentage of mass lost during calcination of the catalyst.

Hoping to gain a better understanding of the surface of the catalysts, XPS was performed on the catalysts synthesized according to Figure 8. These catalysts were analyzed by XPS before calcination in order to examine the surface species immediately after synthesis before oxidation occurs. The samples were stored in a vacuum oven before being transferred to vials. The vials were sealed under a nitrogen atmosphere and then placed in a dessicator that was also sealed under a nitrogen atmosphere before being transported to the X-ray photoelectron spectrophotometer. These measures were taken in order to simulate in-situ analysis as closely as

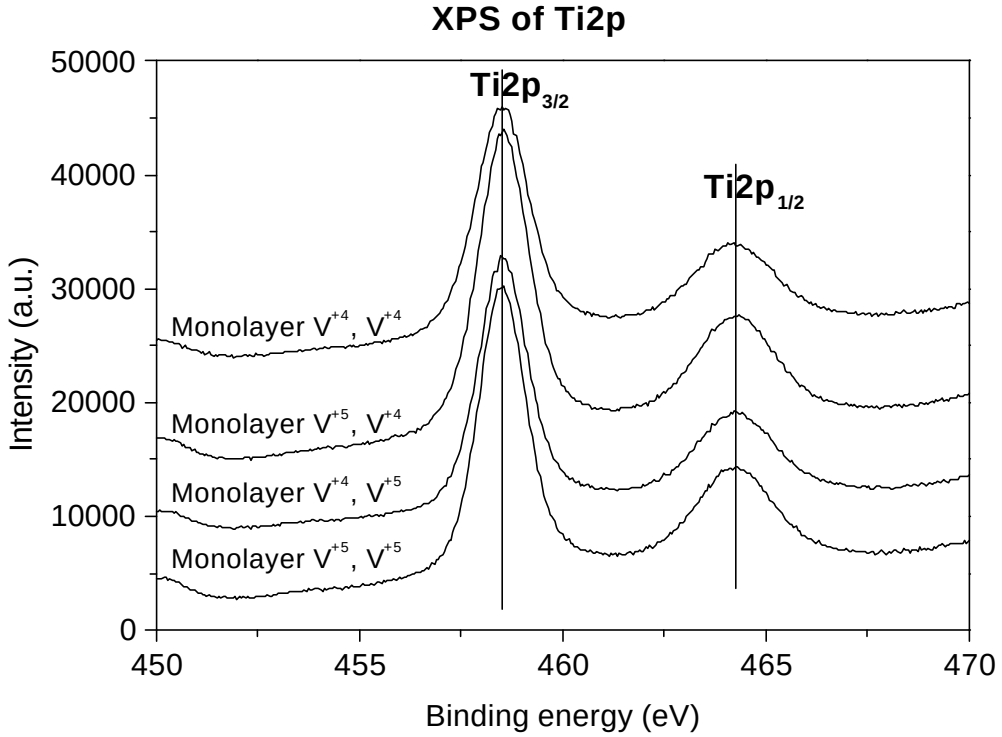

Figure 8. *Ti $2p_{3/2}$ and Ti $2p_{1/2}$ peaks for monolayer coverage of different vanadium loading sequences on P25 TiO_2.*

possible. Figure 9 shows the constant binding energy values observed for the Ti 2p3/2 (458.5 eV) peak, which was used to correct the other XPS spectra through the elimination of charging effects. For all of the XPS spectra presented, the vanadium valence state on the left was applied first at a fraction of monolayer coverage, while the vanadium valence state on the right was applied to achieve theoretical monolayer coverage.

Figure 9. *V $2p_{3/2}$ peaks for monolayer coverage of different vanadium loading sequences on*

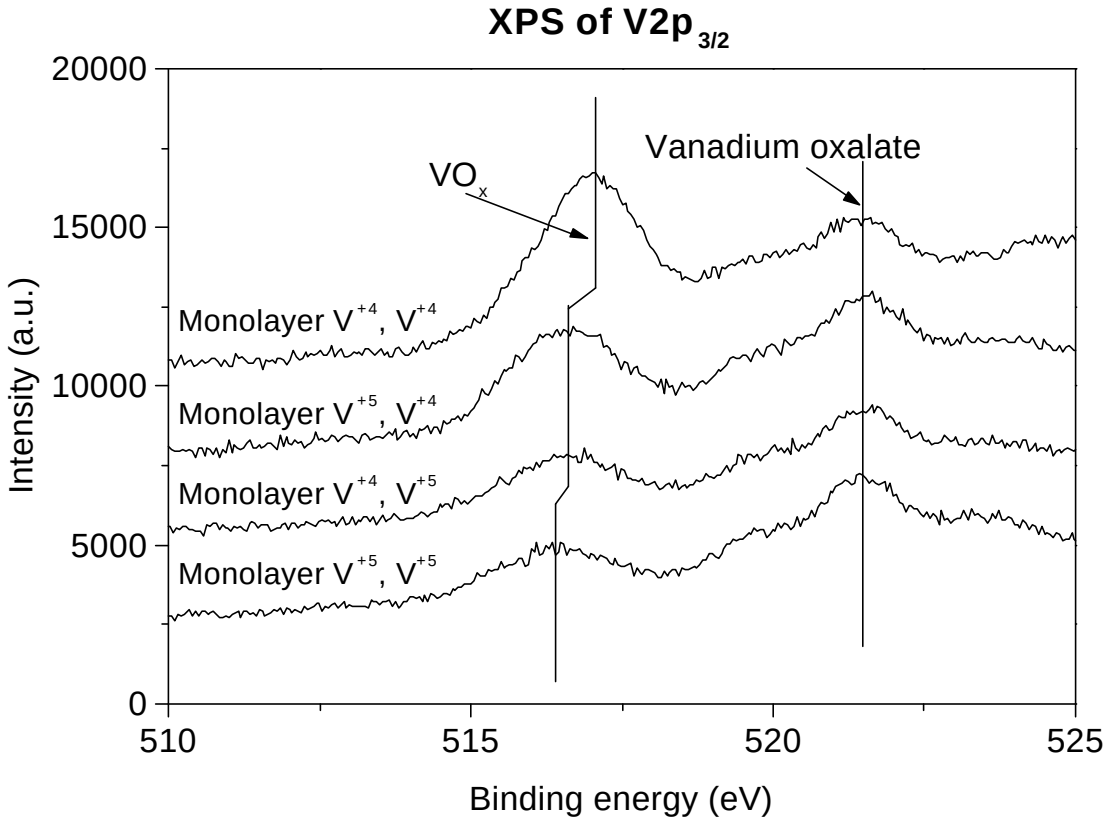

P25 TiO_2.

Figure 9 contains the peaks of analytical interest for the XPS surface study. A noticeable vanadium oxalate peak is present near 522 eV. Because these are uncalcined catalyst samples, it is expected that precursor compounds would not have been completely oxidized and removed. The interesting point to note is for the VO_x peaks. Starting with the two middle samples (V^{+5}, V^{+4} and V^{+4}, V^{+5}), one can observe that the binding energies associated with the maxima of these two peaks is essentially identical. Even though the concentration of the second vanadium species listed in each case is substantially greater than the first one listed, the binding energies for both samples are equal. In other words, the vanadium in these two samples behaves in the same manner. In contrast, the top and bottom spectra (V^{+4}, V^{+4} and V^{+5},V^{+5}) show a difference in binding energies. While the binding energy of the bottom spectrum is close to the values of the middle spectra, it is shifted to a lower energy. Lower binding energies are associated with lower oxidation states (V^{+4}), while higher binding energies are associated with higher oxidation states (V^{+5}). Therefore, it can be seen that the vanadium from the V^{+5} precursor solution is behaving more like V^{+4} once it

is on the catalyst. Looking at the top spectrum, a larger deviation in binding energy from the middle two spectra can be observed. The shift in binding energy of the (V^{+4}, V^{+4}) catalyst, which implies that the vanadium has more V^{+5} rather than V^{+4} character, is greater than the shift in binding energy of the (V^{+5},V^{+5}) catalyst. This is something that was completely unexpected, and there is currently no explanation as to why this occurs. In addition, the surface concentration of vanadium was found to be highest for the (V^{+4}, V^{+4}) catalyst (Table 7).

Table 7. *XPS surface concentrations for monolayer coverage of V_2O_5 on P25 TiO_2*

	Concentration (%)			
Catalyst	V2p	Ti2p	O1s	C1s
Monolayer P25 V4,V4	3.15	12.76	46.96	37.13
Monolayer P25 V4,V5	2.07	13.35	48.43	36.15
Monolayer P25 V5,V5	2.53	15.02	56.17	26.29
Monolayer P25 V5,V4	3.07	16.22	55.74	24.97

That observation leads one to possibly question the distribution of vanadium valence states in the vanadium precursor solution. Even though many references report that V^{+4} in aqueous solutions is blue, while V^{+5} is yellow, perhaps there are other species of vanadium present in the solution. For example, the V^{+4} solution may contain some species of V^{+5} and V^{+3} as well. The distribution of vanadium valence states in the precursor solution may shed some light on the subject. Many spectroscopic methods were used to analyze the aged vanadium oxalate solution. UV-Vis spectroscopy did not provide any means of separation and failed to provide results for the actual aged (blue) vanadium oxalate solution.

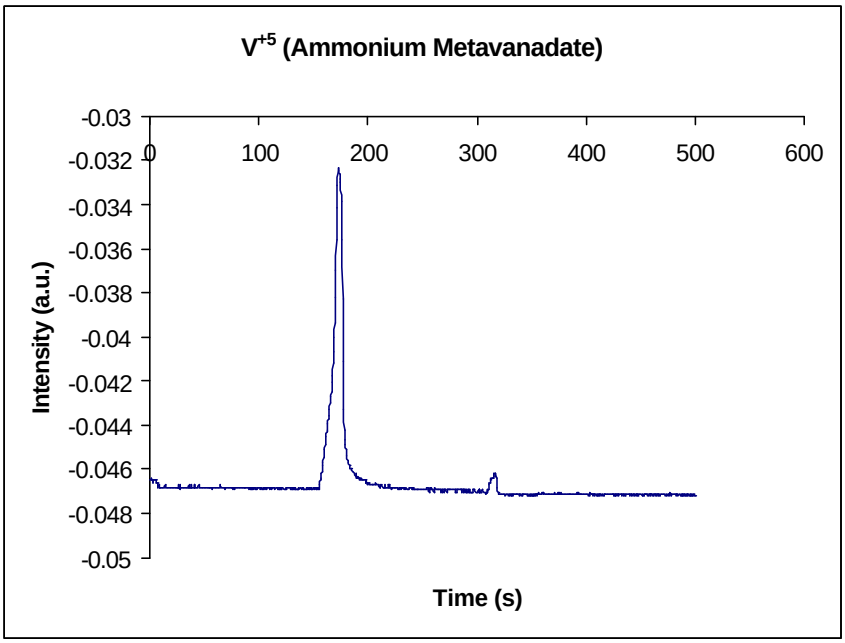

Figure 10. *Capillary electrophoresis spectrum for aqueous ammonium metavanadate*

Capillary electrophoresis, which uses a capillary as resistance and an electrical potential as the driving force to separate ions by different migration times, did provide some initial results for the V^{+5} solution (Figure 10). By its chemical composition (NH_4VO_3), ammonium metavanadate contains V^{+5}. The peak at ~180 seconds should represent that species. However, one can easily notice the other smaller peak that appears near 300 seconds. This peak was not able to be identified but suggests that something else is present. Unfortunately, results could not be obtained for the vanadium oxalate solution (Figure 11). The large shape that appears from ~180-350 seconds is most likely due to a lack of separation in the column or an inability of the UV detector to distinguish between vanadium species attached to different ligands. To check the latter, the same measurement was performed on an Inductively Coupled Plasma Mass Spectrometer. The separation mechanism was unchanged; only the means of detecting the vanadium was different. The results showed approximately 10 different peaks of vanadium compounds migrating over a range of times. That strongly suggested that the separation was indeed occurring and that there are many vanadium complexes that form in the aged vanadium oxalate solution. A potentiometric titration method is currently under development to measure the relative concentrations of V^{+3}, V^{+4}, and V^{+5} in the precursor solution.

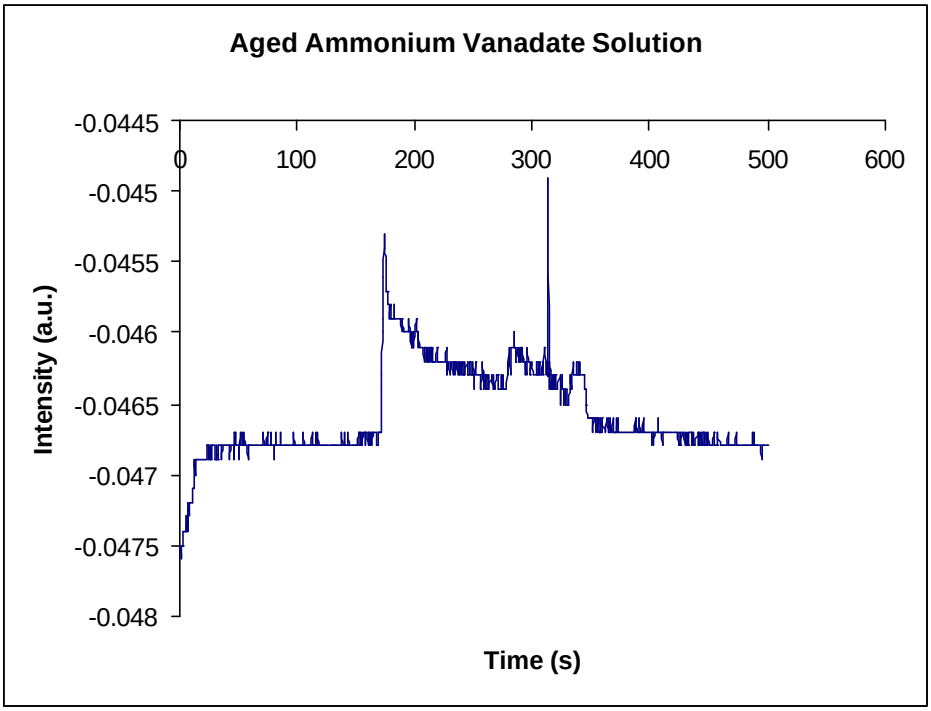

Figure 11. *Spectrum obtained from capillary electrophoresis measurements of the aged vanadium oxalate solution*

2.3 CONCLUSIONS

The surface areas of the supports may play a role in the difference in catalytic performance for different vanadium precursor solutions at extremely high or low values. Vanadium dispersion on the surface of the catalysts is not significantly affected by the valence state of vanadium in the precursor solution. The percentage of mass lost after calcination is also not affected by different

valence states of vanadium, suggesting that the difference in catalytic performance cannot be attributed to the accumulation of a species that may block active sites. XPS results showed that the vanadium species deposited on the support by V^{+4} precursor solution are shifted towards a higher oxidation state (V^{+5}) than by the V^{+5} solution. A number of spectroscopic techniques showed that there is a multitude of vanadium species present in the aged vanadium oxalate solution. Identifying the distribution of vanadium valence states in solution may provide some insight into the observed catalytic performance differences.

III. COMPARISON OF MONOLAYER COVERAGE V_2O_5 CATALYSTS ON DIFFERENT TIO_2 SUPPORTS

ABSTRACT

A number of V_2O_5/TiO_2 catalysts have been tested to study the effect of vanadium's valence state during synthesis for the SCR of NO with NH_3. Monolayer catalysts were synthesized from five different kinds of TiO_2 supports with varying surface areas and crystalline phase compositions. Catalysts prepared from an aged V^{+4} solution consistently performed better than those prepared from fresh V^{+5} solutions. Both NO conversion and N_2 selectivity were improved through the use of V^{+4}. A number of surface characterization techniques were used to search for differences in the properties of catalysts prepared from the two different methods. FT-IR showed that catalysts prepared from V^{+4} possessed both Lewis and Brønsted acid sites before the catalyst was exposed to ammonia. In contrast, V^{+5} possessed only Lewis acid sites before exposure to ammonia. Catalysts synthesized from V^{+4} also showed the presence of stronger acid sites compared to V^{+5}. Those catalysts synthesized from V^{+4} still possessed acidity at temperatures above 300°C**.** H_2 TPR experiments indicated that the reduction of vanadium species deposited as V^{+4} occurs at a lower temperature than vanadium deposited as V^{+5}, suggesting that the increased reducibility of vanadium plays an advantageous role during the redox cycle occurring during this reaction mechanism. Similar to all of the other surface characterization results, Raman spectroscopy revealed no significant differences in the nature of vanadium species present on the surface of the catalysts as a function of the vanadium valence state present during synthesis. The potentiometric titration method was ultimately successful at distinguishing between the V^{+4} and V^{+5} species present in the aged vanadium oxalate solution and showed that the aged solutions are stable over time; little change was seen in the concentration of different vanadium species up to approximately 3 years of storage time.

INTRODUCTION

This section covers the third phase of the project. The work performed during this phase studied the selective catalytic reduction of NO_x. The work primarily aimed at understanding the catalytic differences observed in catalysts synthesized from V^{+4} and V^{+5} solutions through the use of various surface characterization techniques. The catalysts synthesized from V^{+4} were made from a modified vanadia loading procedure developed in our laboratories for the synthesis of TiO_2-based catalysts. A previously synthesized set of catalysts was used to examine the surface characteristics of different vanadium valence states on TiO_2 supports with different properties. A number of characterization techniques were employed to study the surface characteristics of the catalysts and the properties of the vanadium precursor solution. Understanding the role of vanadium's oxidation state during synthesis could lead to the successful manipulation of synthesis parameters to create materials with the catalytic properties necessary for our and other vanadium-based catalyst systems.

3.1 EXPERIMENTAL WORK

3.2.1 Catalyst Preparation

Commercially available titania supports (Table 8) were obtained from various manufacturers based upon their crystalline compositions and surface areas. The supports include: Hombikat TiO_2 from Sachtleben Chemie (99% anatase), P25 TiO_2 from Degussa AG (80% anatase and 20% rutile), TiO_2 from Aldrich (100% anatase) and TiO_2 from Kemira (100% rutile from XRD, Raman experiments show traces of anatase). Vanadium pentoxide was deposited on these supports using aged or fresh vanadium oxalate solutions. Freshly prepared vanadium oxalate solutions made from ammonium metavanadate and oxalic acid were used for V^{+5} synthesis, while identical solutions that had been allowed to age for at least 16 hours were used for V^{+4} synthesis (Economidis et al., 1999). In a typical synthesis, 50 ml of distilled water was added to a 100 ml beaker containing 1.0 g of support. The mixture was heated to 70°C under continuous stirring. Upon reaching 70°C, a measured quantity of vanadium oxalate was added, and the mixture was evaporated to dryness. The paste obtained was further dried overnight at 110°C, ground in a mortar and pestle, and sieved (80 mesh). Calcination of the catalysts was performed at 500°C for 2 hrs in a flow of O_2 (4.2% in helium) at a heating rate of 5°C/min.

Figure 7 illustrates how a subcategory of catalysts was synthesized with multiple valence states of vanadium. First, the required amount of vanadium precursor that would yield approximately 10% of theoretical monolayer coverage was added to the support in the same manner as described above. Second, the catalyst would be dried at 110°C, ground, and sieved through an 80 mesh screen. Third, the vanadium addition procedure would be repeated so that the final catalyst would be covered with enough vanadium to yield theoretical monolayer coverage. Fourth, this final slurry would be dried at 110°C, ground, and sieved through an 80 mesh screen. Calcination of the catalyst would be the next step before catalytic tests.

3.2.2 Characterization

Prior to characterization, the samples were calcined at 500°C for 2 h in O_2 (4.2% in He) at a total flow rate of 20 ml min^{-1}.

Surface Area The specific surface areas of the supports and the catalysts were measured by nitrogen adsorption at 77 K by the BET method using a Micromeritics Gemini 2360. Pore size measurements of various supports were performed using a Micromeritics ASAP 2010. The supports were pretreated *in-situ* at 250°C under vacuum, and the supports were analyzed at 77 K under vacuum.

XRD X-ray diffraction was used to identify and quantify the crystal phases of titania (anatase and rutile) and the crystalline phases of vanadium pentoxide deposited on the various titania supports. XRD studies were performed on a Siemens D500 Diffractometer with a CuK_α radiation source (wavelength 1.5406 Å). Aluminum holders were used to support the samples in XRD measurements. Anatase and rutile phases of titania were determined from the strongest peaks corresponding to anatase [$2\theta = 25.3°$ for the (101) reflection of anatase] and rutile [$2\theta = 27.5°$ for the (110) reflection of rutile]. A combination of Raman and XRD results were used to determine the crystal phases of titania supports. Self-supported pellets (100-150 mg) were used for the Raman study.

XPS X-ray photoelectron spectroscopy was used to analyze the atomic surface concentration on each catalyst. The spectra were recorded on a Perkin-Elmer Model 5300 X-ray photoelectron spectrometer using MgK_α (1253.6 eV) as a radiation source at 300 Watts. The spectra were recorded in the fixed analyzer transmission mode with pass energies of 89.45 and 35.75 eV for recording survey and high-resolution spectra, respectively. The powdered catalysts were mounted onto the sample holder and degassed overnight at room temperature at a pressure on the order of 10^{-7} torr. Binding energies (BE) were measured for C 1*s*, O 1*s*, Ti 2*p*, and V 2*p*. Recorded Auger spectra for V were very weak. Sample charging effects were eliminated by correcting the observed spectra with the Ti $2p_{3/2}$ binding energy (BE) value of 458.5 eV. An estimated error of 0.1 eV can be considered for all the measurements. The spectra were smoothened and a nonlinear background was subtracted. Deconvolution of peaks was done and the fitting was performed using a convolution of Gaussian and Lorenzian curves.

Chemisorption Chemisorption was performed on a Micromeritics ASAP 2010C apparatus with ultra high purity H_2 (Wright Brothers, 99.999%). All samples were degassed at 140 C at atmospheric pressure prior to analysis. Oxygen chemisorption at 370 C was carried out to determine metal dispersion values.

FT-IR FT-IR was used to characterize the acidity of the catalysts. The FT-IR experiments were performed with a Bio-Rad spectrophotometer (FTS-040). Circular self-supporting thin wafers (8 mm diameter) prepared using 8-10 mg catalyst were used for the study. The wafers were placed in a bakeable high-vacuum cell with CaF windows and purged with pre-purified grade helium (30 ml min^{-1}) at 400°C for 2 h to remove any impurities. The sample was cooled down to 150°C, and NH_3 (4.4 vol.% in He) was introduced to the cell and continued flowing (30 ml/min) for a total of 1 h at 150°C to insure complete saturation of the sample. Physisorbed ammonia was removed by flushing the wafer with He for sufficient time. Subsequently, the FT-IR spectra were recorded by desorbing NH_3 at various temperatures ranging from 150-500°C. All the spectra were recorded at 150°C with the aperture set at 2 cm^{-1} to avoid inconsistencies in the results. The data files were then manipulated using Win-IR® and converted into absorbance by taking a ratio of the background spectrum.

H_2-TPR The H_2-TPR experiments were performed on a modified Gow Mac gas chromatograph using 100 mg of calcined catalyst. The catalysts were pretreated at 400°C for 1 h in a pre-purified He (25 ml/min) stream. The furnace temperature was lowered to 50°C, and then the feed containing 6.0 vol% H_2 in He was fed at a flow rate of 25 ml/min. H_2-TPR runs were performed by heating the sample from 50° to 800°C at a linear heating rate of 5°C min^{-1} and keeping the temperature constant for 1 h at 800°C at the end of the run to ensure complete metal oxide reduction. The hydrogen consumed in the TPR was measured quantitatively by a TCD.

3.3 QUANTITATIVE VANADIUM PRECURSOR SOLUTION ANALYSIS

UV/Vis (Ultra Violet/Visible) Spectroscopy Since the oxovanadium complexes present in the precursor solution are so vividly colored, a colorimetric analysis using a UV/Vis spectrophotometer (Shimadzu) was used. The analysis was based upon the principles represented by the following two equations (Fritz and Schenk):

$$A_{\ë1} = å_{A(\ë1)}bc_A + å_{B(\ë1)}bc_B \quad (4)$$

$$A_{\ë2} = å_{A(\ë2)}bc_A + å_{B(\ë2)}bc_B \quad (5)$$

$A_{\ë1 \text{ and }} A_{\ë2}$ are the absorbance of the sample at each particular wavelength ë1 and ë2. $å_{A(\ë1)}$ and $å_{B(\ë1)}$ are the molar absorptivities of species A and species B at wavelength ë1. b is the path length of the cell. c_A and c_B are the concentrations of species A and B, respectively.

3.4 CATALYTIC STUDIES

The SCR of NO with NH_3 at different temperatures at atmospheric pressure was carried out in a fixed bed pyrex reactor (i.d. 6 mm) containing 100 mg of catalyst (80 mesh). Oxygen (Wright Bros., 4.18% in He), ammonia (Matheson, 3.89% in He) and nitric oxide (Air Products, 2.0% in He) were used as received. The inlet concentrations of NO and NH_3 were 2000 ppm, whereas the O_2 concentration was 20,000 ppm (2.0 vol.%). It should be noted that coal-based power plant exhaust contains a much smaller NO concentration (300-400 ppm). The gases were fed at a space velocity (measured at 25°C and 1 atm pressure) of 50,000 h^{-1}. The reaction temperature was measured by a type K thermocouple inserted directly into the catalyst bed. Prior to the catalytic experiments, the catalyst was calcined in oxygen (Wright Bros., 4.18% in He) for 2 hrs at 400°C. The reactants and products were analyzed *on-line* using a Quadrapole mass spectrometer (MKS PPT-RGA). Concentrations of NH_3, N_2, NO, and N_2O were determined by utilizing the cracking patterns of all the gas species present to establish a set of linear equations that could be solved to determine the real concentration of gas species without the interference of fragments. The definitions used for NO conversion and nitrogen selectivity are shown in Equations 6-7:

$$\text{NO conversion} = 100 \times [(NO_{in} - NO_{out})/NO_{in}] \quad (6)$$

$$N_2 \text{ selectivity} = 100 \times [N_2/(N_2 + N_2O)] \quad (7)$$

3.5 RESULTS AND DISCUSSION

A number of TiO_2 supported V_2O_5 catalysts were synthesized to study the impact of vanadium's valence state during synthesis on the catalytic performance of these materials during the selective catalytic reduction of nitric oxide with ammonia. The properties of these catalysts are shown in Table 8. While the results have not been finalized yet because of interference from other species, the aged vanadium solution consists of approximately 90% V^{+4} and 10% V^{+5} as determined by UV/Vis spectroscopy.

Table 8. *Physical properties of catalysts used in this study*

Support	V_2O_5 wt%	V Valence State during Synthesis	XRD A:R Support	BET S.S.A. (m^2/g) Support	BET S.S.A. (m^2/g) Catalyst	Dispersion (%)	Crystallite Size (nm)
TiO_2 (S)	10	5+	A	309	n.d.	48	n.p.
TiO_2 (S)	10	4+	A	309	n.d.	52	n.p.
TiO_2 (S)	22	5+	A	309	16	29	27.5
TiO_2 (S)	22	4+	A	309	15.9	30	28.5
TiO_2 (S)	45	5+	A	309	n.d.	n.d.	27.1
TiO_2 (S)	45	4+	A	309	n.d.	24	26.2
TiO_2 (I)	5	5+	A	63	51.8	55	n.p.
TiO_2 (I)	5	4+	A	63	53.3	57	n.p.
TiO_2 (K)	4	5+	R	52	42.2	47	n.p.
TiO_2 (K)	4	4+	R	52	42.1	36	n.p.
TiO_2 (D)	4	5+	A:R 80:20	51	44.6	38	n.p.
TiO_2 (D)	4	4+	A:R 80:20	51	51	39	n.p.
TiO_2 (A)	1	5+	A	9	10.1	29	n.p.
TiO_2 (A)	1	4+	A	9	9.9	38	n.p.

A: anatase, R: rutile, n.p.: no V_2O_5 peaks present, n.d.: not determined
S: Sachtleben Chemie Hombikat UV 100, I: Ishihara, K: Kemira, D: Degussa P25, A: Aldrich

It has been shown that the valence state of vanadium during the synthesis of TiO_2 supported monolayer V_2O_5 catalysts significantly affects catalytic performance (Figure 12). The activity of V_2O_5 catalysts synthesized from an aged vanadium oxalate solution (V^{+4}) is higher than catalysts made from fresh vanadium oxalate solutions (V^{+5}). At 300°C and 50,000 h^{-1}, one can observe that the greatest enhancement in performance occurs on the Hombikat TiO_2 support. The smallest difference in activity is seen on Aldrich TiO_2. In fact, it is the only support on which V^{+5} performs better than V^{+4}. However, since the catalytic activity of this support is negligible anyway, the contrary results are insignificant for all practical purposes. The poor performance of V_2O_5 supported on Aldrich TiO_2 can be attributed to the almost nonexistent acidity and hence activity of the support. Examining figure 13, which plots catalytic performance as a function of temperature, shows that monolayer catalysts supported on Ishihara ST-21 TiO_2 offer superior performance when compared to all the other catalysts. Both Ishihara and Hombikat TiO_2 seem to shift the optimum activity of monolayer V_2O_5 catalysts down to lower temperatures, as seen by

their decrease in NO conversion at temperatures above 300°C (Figure 13). An interesting trend observed in this figure is the difference in activity between the V^{+4} and V^{+5} catalysts as a function of temperature. Monolayer catalysts on each of the supports that are synthesized from V^{+4} provide almost identical performance at lower temperatures (250-300°C). As the temperature increases, it can be seen that Ishihara maintains its performance, while the activity of Hombikat sharply decreases with an increase in temperature. This can be attributed to the tendency of V_2O_5/Hombikat TiO_2 catalysts to oxidize ammonia at higher temperatures (not shown). This essentially uses up the reactant and is reflected in the conversion results of the catalyst.

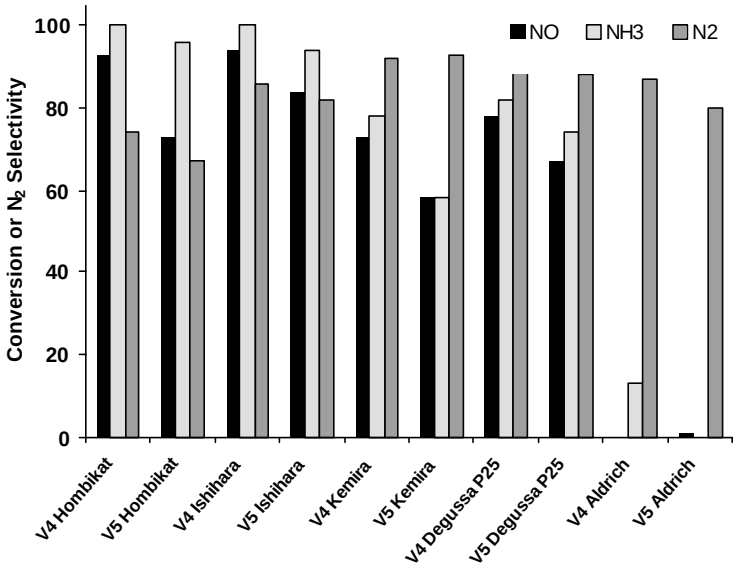

Figure 12. *Catalytic performance of monolayer V_2O_5/TiO_2 catalysts supported on different types of TiO_2 supports at 300°C and 50,000 h^{-1}*

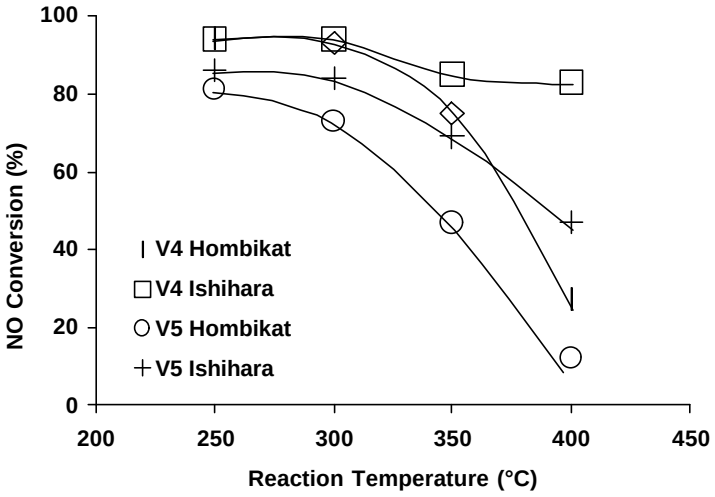

Figure 13. *Catalytic performance of monolayer coverage of V_2O_5 on Hombikat and Ishihara TiO_2 supports*

Both NO conversion and N_2 selectivity are higher in catalysts synthesized from V^{+4} compared to V^{+5}. Characterization techniques revealed some significant differences in the properties of catalysts synthesized from the two different methods. Catalysts synthesized from V^{+4} start with both Brϕnsted and Lewis acid sites, while those synthesized from V^{+5} initially only possess Lewis acid sites (Figure 14). This lends support to suggested mechanisms where Brϕnsted acid sites play a major role.

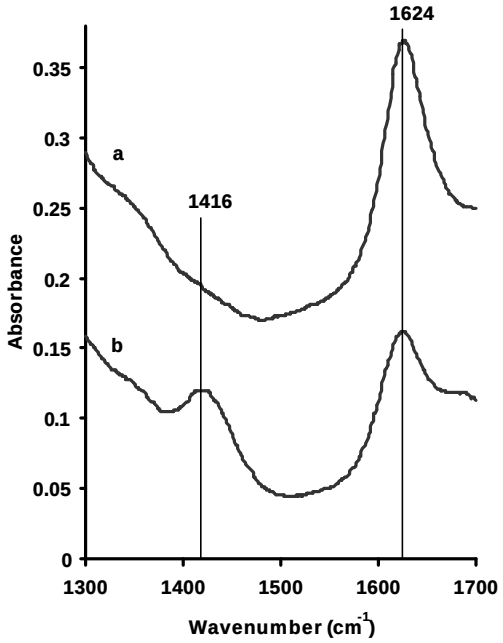

Figure 14. *FT-IR spectra of uncalcined 22.4 wt.% V_2O_5/ Hombikat TiO_2 synthesized by a) V^{+5} or b) V^{+4} recorded at room temperature in helium.*

Some researchers have concluded that the reduction of NO_X with NH_3 on crystal V_2O_5 surfaces proceeds through the participation of Brønsted acid sites (Gasior et al., 1988 and Odriozola et al., 1989). In addition they have shown that NO can adsorb on reduced vanadia and titania, demonstrating that the titania support can play an important role in SCR reactions (Odriozola et al., 1989). Supporting results were published using vanadia/titania (V_2O_5/TiO_2) aerogels. In this case, Brønsted acidity was shown to facilitate the reduction of NO to N_2, and catalytic activity improved as vanadia content increased (Schneider et al., 1994). In contrast, it has been shown that unsaturated V^{4+} oxovanadyls are the active sites for the reduction of NO (Ciambelli et al., 1989). Those unsaturated species act as Lewis acid sites and prevail at low vanadia concentrations. V^{5+} oxo-hydronal groups, whose concentrations increase with V_2O_5 content until monolayer coverage is achieved, are less active in the transformation of NO to N_2. In contrast, they favor the unwelcome formation of nitrous oxide (Kotter et al., 1989). It is evident from these reports that the product selectivity for the SCR of NO_x depends on the type and concentration of vanadyl species. The Lewis acidity associated with the anatase phase of titania also increases the transformation of NO to undesired nitrous oxide. In fact they concluded that TiO_2 could decrease catalytic performance because it forms a strong bond with adsorbed ammonia (Morterra et al., 1980). Additionally, it was concluded that ammonia can strongly adsorb on the V-OH sites, which are important sites for the $DeNO_x$ reaction (Topsøe, 1991; 1994). The adsorption of ammonia on these sites hinders the $DeNO_x$ performance of the catalysts. Therefore, a catalyst that decreases

ammonia adsorption on the V-OH sites would be desirable because more sites would be available to carry out the $DeNO_x$ reaction.

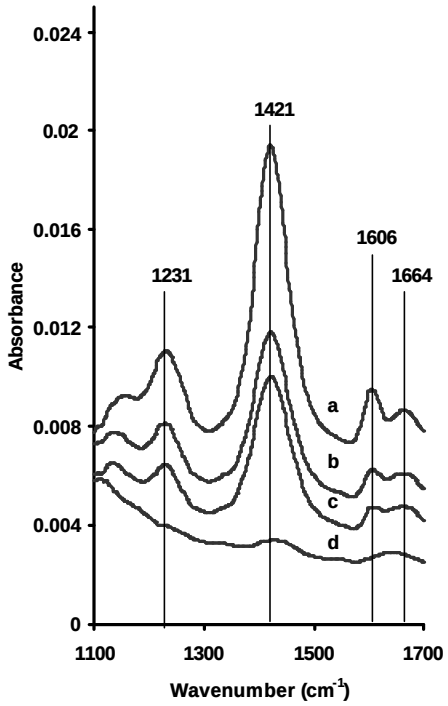

Figure 15. *FT-IR spectra of 22.4 wt% V_2O_5/Hombikat TiO_2 synthesized from V^{+4}. a) 150°C, b) 250°C, c) 300°C, d) 350°C (Calcined at 500°C for 2 hours, pretreated for 2 hours at 400°C in helium, all samples cooled to 150°C for data collection)*

In addition to the initial possession of Brϕnsted acid sites on V^{+4} catalysts, the catalysts also possess another advantage. Their acid sites are stronger, as Brϕnsted and Lewis acid peaks (1421 and 1606 cm^{-1}, respectively) are still visible at temperatures above 300°C during NH_3-FT-IR analysis (Figures 15, 16). Figure 15 shows the higher acidity of V4 Hombikat, as peaks resulting from ammonia adsorption are still visible at temperatures as high as 350°C. The absence of peaks beginning at 300°C in Figure 16 demonstrates the weaker acidity of V5 Hombikat. This trend was consistent for all catalysts studied. As a result, some type of surface complex may be depositing during the synthesis process that produces these favorable performance advantages. The effects of this proposed surface complex are seen even after the catalyst has been calcined at 500°C for 2 hours in oxygen.

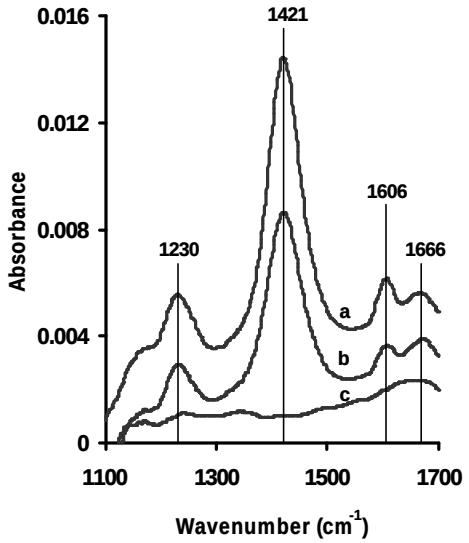

Figure 16. *FT-IR spectra of 22.4 wt% V_2O_5/Hombikat TiO_2 synthesized from V^{+5}. a) 150°C, b) 250°C, c) 300°C (Calcined at 500°C for 2 hours, pretreated for 2 hours at 400°C in helium, all samples cooled to 150°C for data collection)*

The beneficial effects of V^{+4} on surface acidity are observed on the sequentially layered catalysts supported on P25 as well. These catalysts were synthesized according to the procedure depicted in Figure 7. Figure 16 shows the similar trend observed over Hombikat TiO_2 with a monolayer of V_2O_5.

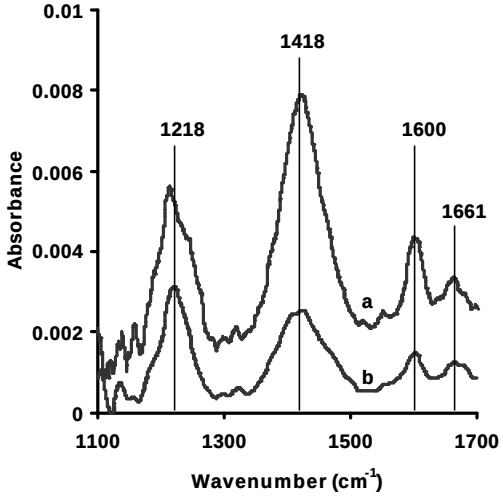

Figure 17. *FT-IR spectra of 7.25 wt% V_2O_5/P25 TiO_2. Initial layer V^{+4}. Final layer V^{+5}. a) 150°C, b) 250°C, c) 300°C (Calcined at 500°C for 2 hours, pretreated for 2 hours at 400°C in helium, all samples cooled to 150°C for data collection)*

Ammonia adsorption peaks have disappeared by 300°C, indicating the weaker acidity of this catalyst.

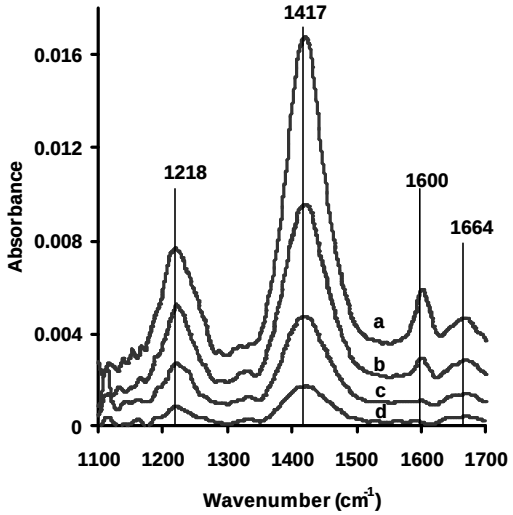

Figure 18. *FT-IR spectra of 7.25 wt% V_2O_5/P25 TiO_2. Initial layer V^{+5}. Final layer V^{+4}. a) 150°C, b) 250°C, c) 300°C, d) 350°C (Calcined at 500°C for 2 hours, pretreated for 2 hours at 400°C in helium, all samples cooled to 150°C for data collection)*

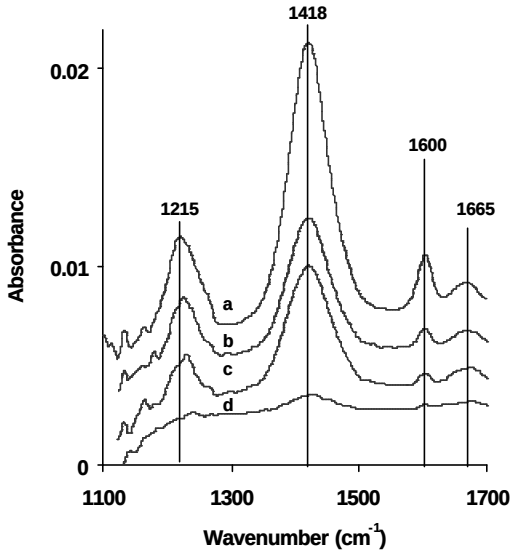

Figure 19. *FT-IR spectra of 7.25 wt% V_2O_5/P25 TiO_2. Initial layer V^{+4}. Final layer V^{+4}. a) 150°C, b) 250°C, c) 300°C, d) 350°C (Calcined at 500°C for 2 hours, pretreated for 2 hours at 400°C in helium, all samples cooled to 150°C for data collection)*

The SCR process has been well studied, and Bronsted acid sites have been shown to participate in an oxidation-reduction cycle. With the acidity aspects examined, it was only natural to look at the other area of the mechanism. The reducibility of the active metal component of the catalyst is slightly increased by synthesis with V^{+4} as opposed to V^{+5}. It is quite possible that this shift in reducibility towards lower temperatures contributes to the performance advantage of V^{+4} vs. V^{+5} catalysts.

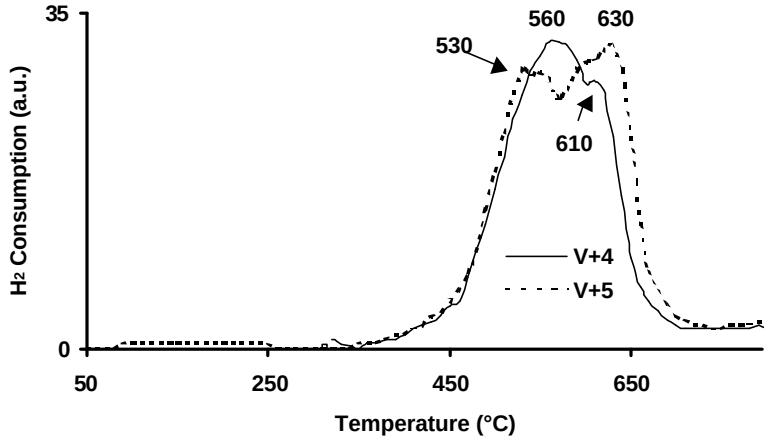

Figure 20. *Hydrogen temperature programmed reduction of 22.4 wt% V_2O_5/Hombikat TiO_2 synthesized from V^{+4} and V^{+5}. (50-800°C at 5°C/min, dwell at 800°C for 1 hour)*

No real discrepancies could be found between the two synthesis methods using the other analysis techniques. BET surface area, mass loss during calcination, and XPS data were all quite similar. Specifically, XPS results showed that there really were not any significant differences in surface concentrations of vanadium for the oxidation states of the vanadium species present on the catalysts. Additionally, no differences were observed in vanadium metal dispersion values, indicating that the possible surface species present during synthesis that may lead to performance enhancements do not affect the nature of the interaction between the active metal and the support. Crystallite sizes were also calculated (Table 8) using Scherrer's equation for Hombikat TiO_2 supported catalysts containing one and two monolayers. These particular catalysts were chosen because of the relatively weak XRD signal for V_2O_5 (Figure 20). As seen in the table, all of the measured crystallite sizes are in the vicinity of 27 nm and do not provide statistically different results. In addition to the methods mentioned above, Raman spectroscopy was also used to examine the surface of the catalysts at ambient conditions. Similar to all of the other surface characterization results, Raman spectroscopy revealed no significant differences in the nature of vanadium species present on the surface of the catalysts as a function of the vanadium valence state present during synthesis (Figures 21,22). The potentiometric titration method was ultimately successful at distinguishing between the V^{+4} and V^{+5} species present in the aged vanadium oxalate solution and showed that the aged solutions are stable over time; little change was seen in the concentration of different vanadium species up to approximately 3 years of storage time (Figure 23).

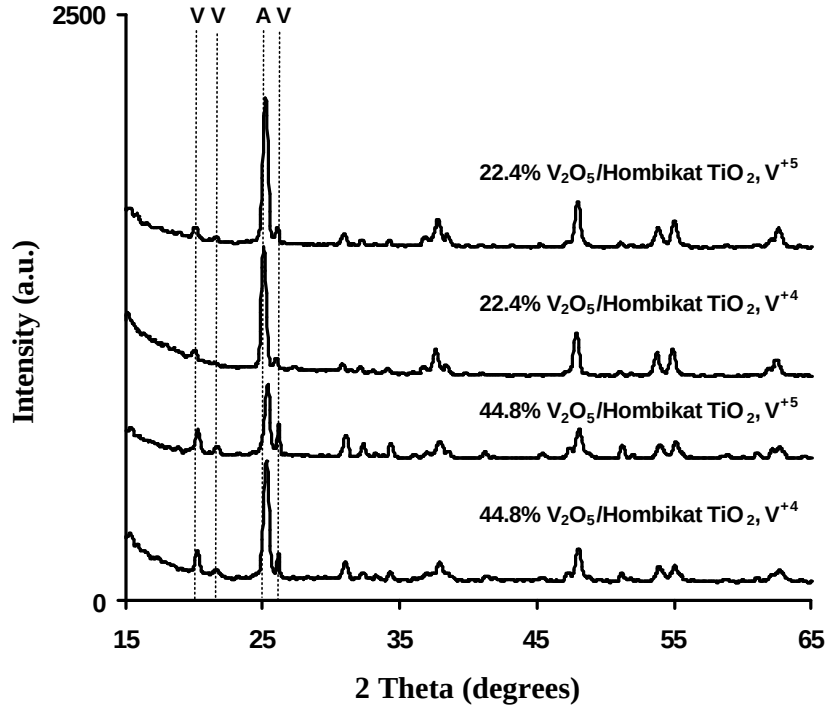

Figure 21. *XRD spectra of single and double monolayer V_2O_5 catalysts.*

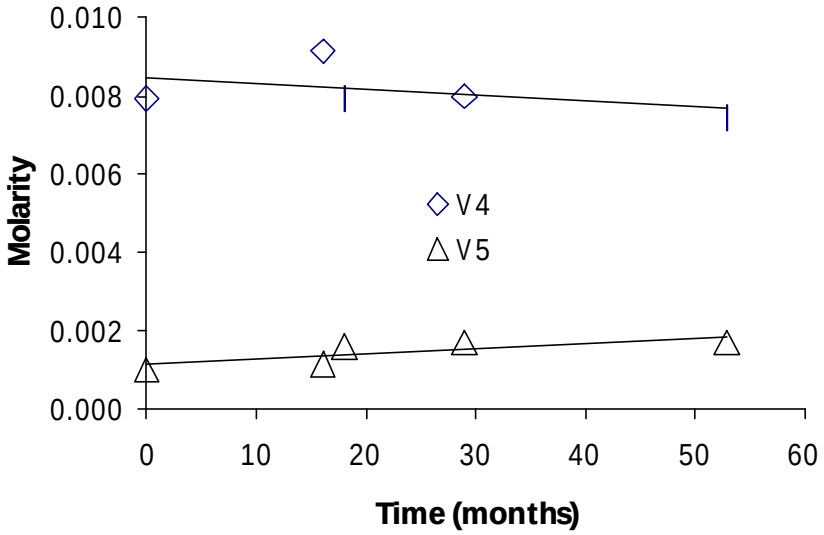

Figure 22. *Distribution of V^{+4} and V^{+5} ions in the aged vanadium oxalate solution over time.*

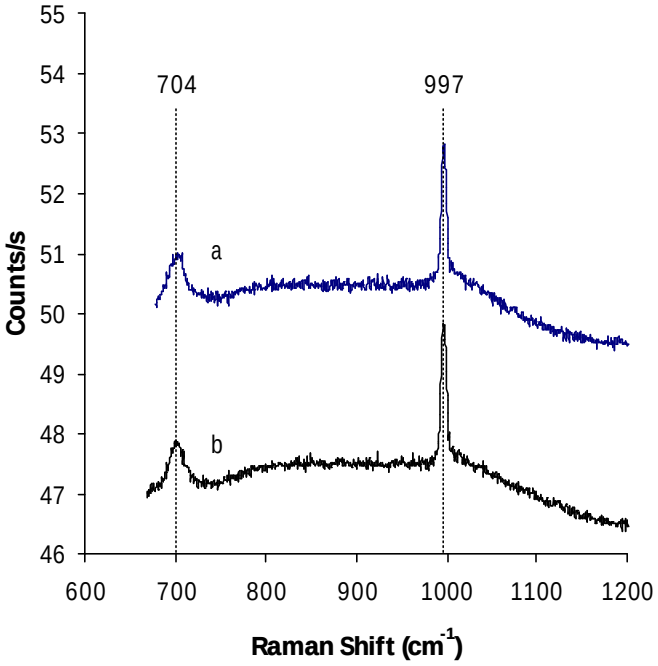

Figure 23. *Raman spectra collected under ambient conditions for (a) 22.4 wt% V_2O_5/Homibat TiO_2 synthesized with V^{+4} and (b) 22.4 wt% V_2O_5/Homibat TiO_2 synthesized with V^{+5}.*

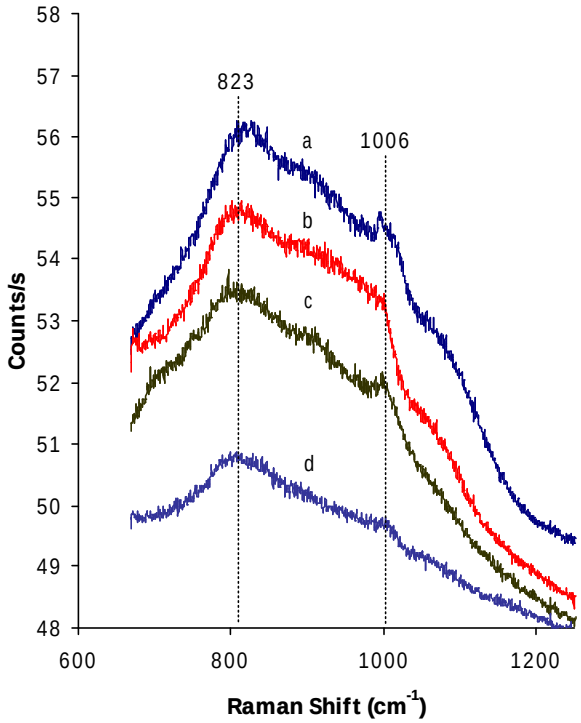

Figure 24. *Raman spectra collected under ambient conditions of 7 wt% V_2O_5/P25 TiO_2: (a) V^{+5} initial layer, V^{+5} completion of monolayer, (b) V^{+4} initial layer, V^{+5} completion of monolayer, (c) V^{+4} initial layer, V^{+4} completion of monolayer, and (d) V^{+5} initial layer, V^{+4} completion of monolayer.*

3.6 CONCLUSIONS

It has been shown that the valence state of vanadium during the synthesis of TiO_2 supported monolayer V_2O_5 catalysts significantly affects catalytic performance. Both NO conversion and N_2 selectivity are higher in catalysts synthesized from V^{+4} compared to V^{+5}. Characterization techniques revealed some significant differences in the properties of catalysts synthesized from the two different methods. Catalysts synthesized from V^{+4} start with both Brønsted and Lewis acid sites, while those synthesized from V^{+5} initially only possess Lewis acid sites. This lends support to suggested mechanisms where Brønsted acid sites play a major role. In addition to the initial possession of Brønsted acid sites on V^{+4} catalysts, V^{+4} catalysts also possess another advantage. Their acid sites are stronger, as Brønsted and Lewis acid peaks are still visible at temperatures above 300°C during NH_3-FT-IR analysis. As a result, some type of surface complex may be depositing during the synthesis process that produces these favorable performance advantages. The effects of this proposed surface complex are seen even after the catalyst has been calcined at 500°C for 2 hours in oxygen.

The reducibility of the active metal component of the catalyst is slightly increased by synthesis with V^{+4} as opposed to V^{+5}. It is quite possible that this change in reproducibility has profound implications in the redox mechanism of this reaction. No real discrepancies could be found between the two synthesis methods using the other analysis techniques. BET surface area, mass loss during calcination, and XPS data were all quite similar. Specifically, XPS results showed that there really were not any significant differences in surface concentrations of vanadium for the oxidation states of the vanadium species present on the catalysts. Similar to all of the other surface characterization results, Raman spectroscopy revealed no significant differences in the nature of vanadium species present on the surface of the catalysts as a function of the vanadium valence state present during synthesis. The potentiometric titration method was ultimately successful at distinguishing between the V^{+4} and V^{+5} species present in the aged vanadium oxalate solution and showed that the aged solutions are stable over time; little change was seen in the concentration of different vanadium species up to approximately 3 years of storage time. Additionally, no differences were observed in vanadium metal dispersion values, indicating that the possible surface species present during synthesis that may lead to performance enhancements do not affect the nature of the interaction between the active metal and the support.

5. REFERENCES

J. L. Alemany, L. Lietti, N. Ferlazzo, P. Forzatti, G. Busca,,E. Giamello, and F. Bregani, *J. Catal.* **155** (1995) 117.

M. D. Amiridis, B. K. Na, and E. I. Ko, 207th National ACS Symposium Series, San Diego, March 13-18, 1994, pp. 116-120.

G. C. Bond and K. Brückman, *Faraday Disc. Chem. Soc.* **72** (1981) 1071.

G. C. Bond and S. F. Tahir, *App. Catal.* **71** (1991) 1.

P. Ciambelli, G. Bagnasco, L. Lisi, M. Turco, G. Chiarello, M. Musci, M. Notaro, and D. Rodda, *App. Catal.* **52**, (1989) 225.

R. J. H. Clark, The chemistry of titanium and vanadium, Elsevier, London, 1968.

C. Cristiani, M. Belloto, P. Forzatti, and F. Bregani, *J. Mater. Res.* **8** (1993) 2019.

H. E. Curry-Hyde and A. Baiker, *Ind. Eng. Chem. Res.* **29** (1990) 1985.

N. Economidis, R. Coil, and P. Smirniotis, *Catal. Today* **40** (1998) 27.

N. V. Economidis, D. A. Peña, and P. G. Smirniotis, *Applied Catalysis B: Environmental* **23** (1999) 123-134

J. S. Fritz and G. H. Schenck, G.H., Jr., *Quantitative Analytical Chemistry,* (1969).

M. Gasior, J. Haber, T. Machez, T. Czeppe, *J. Mol. Catal.*, **43**, (1988) 359.

L. Gordon, M. L. Salutsky, and H. H. Willard, *Precipitation from homogeneous solution*, Wiley & Sons, London, 1959.

B. E. Handy, A. Baiker, A., M. Schraml-Marth, and A. Wokaun, *J. Catal.* **134** (1992) 21.

I. M. Kolthoff, R. Belcher, V. A. Stenger, G. Matsuyama, *Volumetric Analysis Volume III Titration Methods: Oxidation-Reduction Reactions*, New York: Interscience Publishers, 1957.

M. Kotter, H.G. Lintz, T. Turek, and D. L. Timm, *App. Catal.*, **52**, (1989) 225.

L. Lietti, J. Svachula, P. Forzatti, G. Busca, G. Ramis, and F. Bregani, *Catal. Today* **17** (1993) 131.

L. Lietti, J.L. Alemany, P. Forzatti, G. Busca, G. Ramis, E. Giamello, and F. Bregani, *Catal. Today* **29** (1996) 143.

C. Morterra, G. Ghiotti, and E. Garrone, *J. Chem. Soc. Faraday I* **76** (1980) 2102.

J. A. Odriozola, H. Heinemann, G.A. Somorjai, J. F. G. De la Banda, and P. J. Pereira, *J. Catal.* **119**, (1989) 71.

G. Ramis, G. Busca, and P. Forzatti, *Appl. Catal. B:Environmental* **1** (1992) L9.

G. Ramis, G. Busca, C. Cristiani, L. Lietti, P. Forzatti, and F. Bregani, *Langmuir* **8** (1992) 1744.

F. Roozeboom, M. C. Mittelmeijer-Hardeger, J. A. Moulijin, J. Medena, V. H. J. de Beer, and P. J. Gellings, *J. Phys. Chem.* **84** (1980) 2783.

G. M. Robb, W. Zhang, and P. G. Smirnotis, *Microporous and Mesoporous Materials*, **20** (1998) 307.

H. Schneider, S. Tschudin, M. Schneider, A. Wokaun, A. Baiker, *J. Catal.* **147**, (1994) 5.

J. Selbin, *Chemical Reviews*, **65** (1965) 153-175.

R. A. Spurr, and H. Myers, *Analytical Chem.* **29** (1957) 760.

K. Tanabe, M. Misono, Y. Ono, H. Hattori, *New Solid Acids and Bases*, Vol 51., New York: Elsevier Science Publishers, 1989.

N.-Y. Topsøe, *J. Catal*., **128**, (1991) 499.

N.-Y. Topsøe, *Science* **265** (1994) 1217.

N.-Y. Topsøe, J. A. Dumesic, and H. Topsøe, *J. Catal.* **151** (1995a) 241.

N.-Y. Topsøe, H. Topsøe, and J. A. Dumesic, *J. Catal.*, **151** (1995b) 226.

A. Vogt, A. J. Boot, A. Van Dellen, J. W. Geuss, F. J. J. G. Janssen, and F. M. G. Van Den Kerkhof, *J. Catal*. **114** (1988) 313.

I. E. Wachs, G. Deo, B. M. WeckHuysen, A. Andreini, M. A. Vuurman, M. d eBoer, and M. D. Amiridis, *J. Catal*. **161** (1996) 24.

G. T. Went, S. T. Oyama, and A. T. Bell, *J. Phys. Chem.* **94** (1990) 4240.

G. T. Went, L.-J. Leu, and A. T. Bell, *J. Catal.* **134** (1992a) 479.

D. Wang, H. H. Kung, and M. A. Barteau, *Applied Catalysis A: General* **201** (2000) 203-213

Refereed Articles, Presentations, and Students Receiving Support from the Grant

International Journal Articles (peer reviewed)

1) Economidis N. V., Peña, D. A., and Smirniotis, P. G. "Comparison of TiO_2-based Oxide Catalysts for the Selective Catalytic Reduction of NO: Effect of Aging the Vanadium Precursor Solution", **Applied Catalysis B: Environmental,** Vol. 23, 123-134, 1999.

2) Uphade, B., Peña D.A., Jenkins, R.G., and Smirniotis, P.G., "On the Unusual Behavior of Transition Metal Oxides supported on Ishihara TiO_2 (ST-21) in the Low-Temperature SCR of NO with NH_3", in preparation for submission to **Catalysis Communications,** 2002.

3) Peña, D. A., Reddy, E.P., Jenkins, R. G., and Smirniotis, P. G. "DeNOx Catalysts with Controlled Valence of Vanadium for Optimum SCR Performance", to be submitted to **Journal of Catalysis** , 2002.

4) Peña, D. A., Jenkins, R. G., and Smirniotis, P. G. "Investigation of Ultrathin Vanadium Layers on TiO_2 Support under Reductive and Oxidative Atmospheres", to be submitted to **Journal of Catalysis** , 2002.

5) Peña, D. A., Jenkins, R. G., and Smirniotis, P. G. "Effect of Oxide Supports loaded with V^{4+} Species for SCR Reactions", in preparation for submission to **Applied Catalysis B: Environmental,** 2002.

Conference Presentations

1) Peña D. A., Jenkins, R. G., and Smirniotis, P. G. "Investigation of the Valence State of Vanadium during Impregnation for the SCR of NO using NH_3", presented at The Tri-State Catalysis Society Spring Symposium, Louisville, KY, April 20-21, 1999.

2) Peña D. A., Jenkins, R. G., and Smirniotis, P. G. "The Role of V Valence State in the Precursor Solution of DeNOx Catalysts", presented at The 16th North American Meeting of the Catalysis Society, Boston, MA, May 30-June 3, 1999.

3) Peña D. A., Jenkins, R. G., and Smirniotis, P. G. "Investigation of the Valence State of Vanadium during Impregnation for the SCR of NO using NH_3", The 2000 Annual AIChE Meeting in Los Angeles, CA, November 12-17, 2000.

4) Peña D. A., Jenkins, R. G., and Smirniotis, P. G. "Characterization and Reactivity of V_2O_5/TiO_2 SCR Catalysts Synthesized from $V^{(IV)}$ or $V^{(V)}$ Solutions", (poster) The 2001 Annual AIChE Meeting in Reno, NV, November 4-9, 2001

5) Peña D. A., Jenkins, R. G., and Smirniotis, P. G. "Interaction of Vanadium Species on TiO_2-supported SCR Catalysts" ICCS, October 2001, Rescheduled

Students who have received support from the grant.

Graduate Students:

1) Mr. Donovan Peña, graduate (Ph.D.) student in Chemical Engineering
2) Mrs. Elizabeth Allen, graduate (M.S.) student in Chemical Engineering
3) Mr. Tianxin Zhang, graduate (M.S.) student in Chemical Engineering